

軟X線磁気円二色性によるスピントロニクス材料の研究

藤森 淳

東京大学理学系研究科

分光測定

片岡隆史, Vijay Raj Singh, 山崎陽, 小林正起(東大理・新領域)

小出常晴, 朝倉大輔, 間宮一敏(物構研PF)

竹田幸治, 岡根哲夫, 大河内拓雄, 斎藤祐児(原子力機構)

F.-H. Chang, C.-S. Yang, L. Lee, H.-J. Lin, D.-J. Huang, C.T. Chen (NSRRC, Taiwan)

試料

田中雅明, 大矢 忍, ファムナムハイ(東大工) $Ga_{1-x}Mn_xAs$

福村知昭, 山田 良則, 上野 和紀, 川崎雅司(東北大金研・WPI材料機構) $Ti_{1-x}Co_xO_2$

黒田眞司, 石川弘一郎, 張 珂(筑波大物質工) $Zn_{1-x}Cr_xTe$

K.V. Rao, M. Kapilashrami, L. Belova (Royal Inst Tech, Swedem) $Zn_{1-x}Mn_xO$ 薄膜

D. Karmakar (BARC), S.K. Mandal, T.K. Nath (IIT Kharagpur), I. Dasgupta (IACS)

$Zn_{1-x}Fe_xO$, $Zn_{1-x}(Fe, Co)_xO$, $Zn_{1-x}(Mn, Co)_xO$ ナノ粒子

理論

田中 新(広大先端物質) 多重項計算, クラスタ計算

Discovery of ferromagnetism in MBE-grown Mn-doped III-V-based DMS

VOLUME 63, NUMBER 17

PHYSICAL REVIEW LETTERS

23 OCTOBER 1989

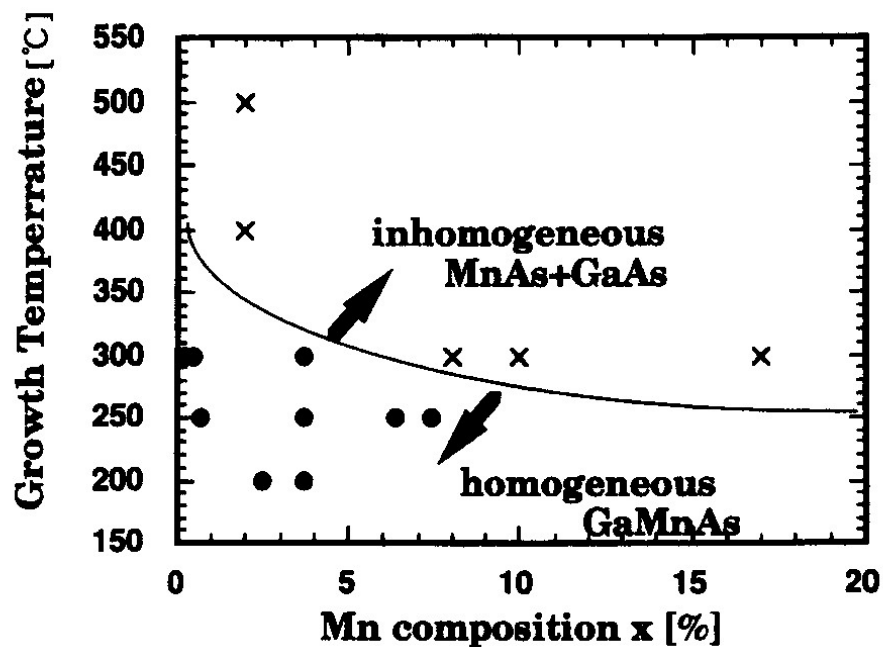
Diluted Magnetic III-V Semiconductors

H. Munekata, H. Ohno,^(a) S. von Molnar, Armin Segmüller, L. L. Chang, and L. Esaki

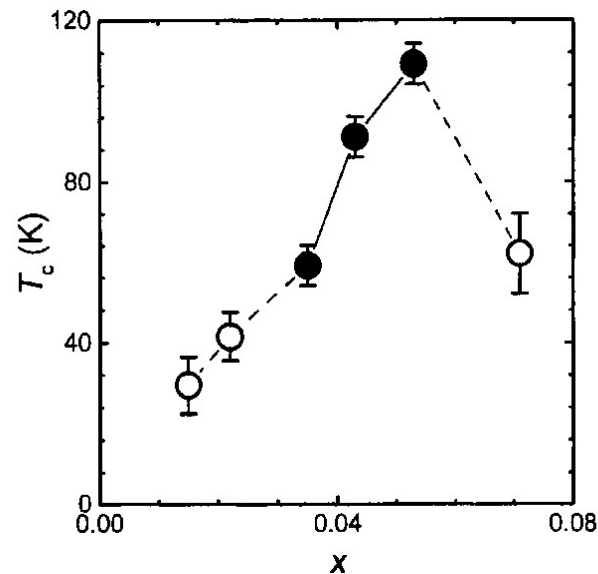
IBM T. J. Watson Research Center, P.O. Box 218, Yorktown Heights, New York 10598

(Received 8 August 1989)

Growth "phase diagram" of $\text{Ga}_{1-x}\text{Mn}_x\text{As}$ Curie temperature of $\text{Ga}_{1-x}\text{Mn}_x\text{As}$

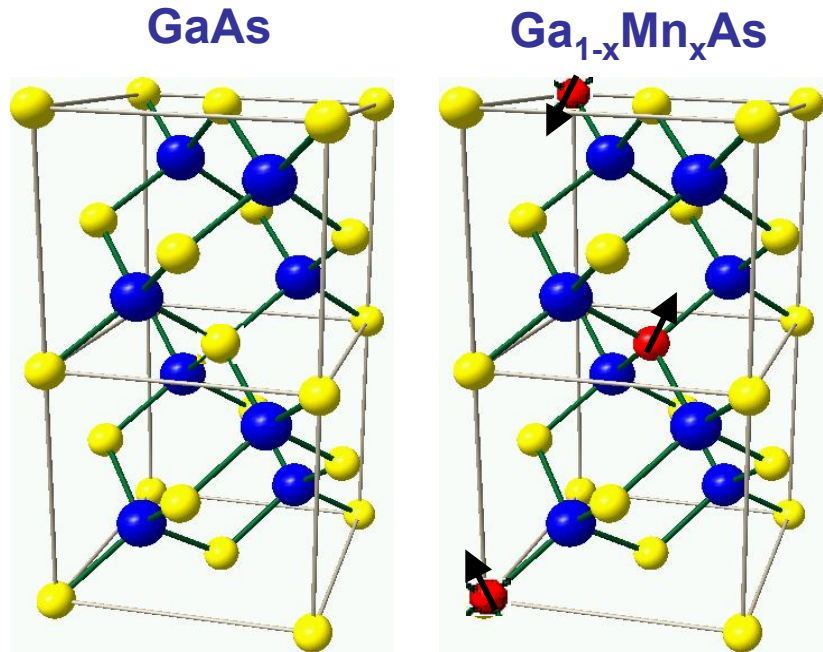


T. Hayashi, M. Tanaka, J. Cryst. Growth, '97

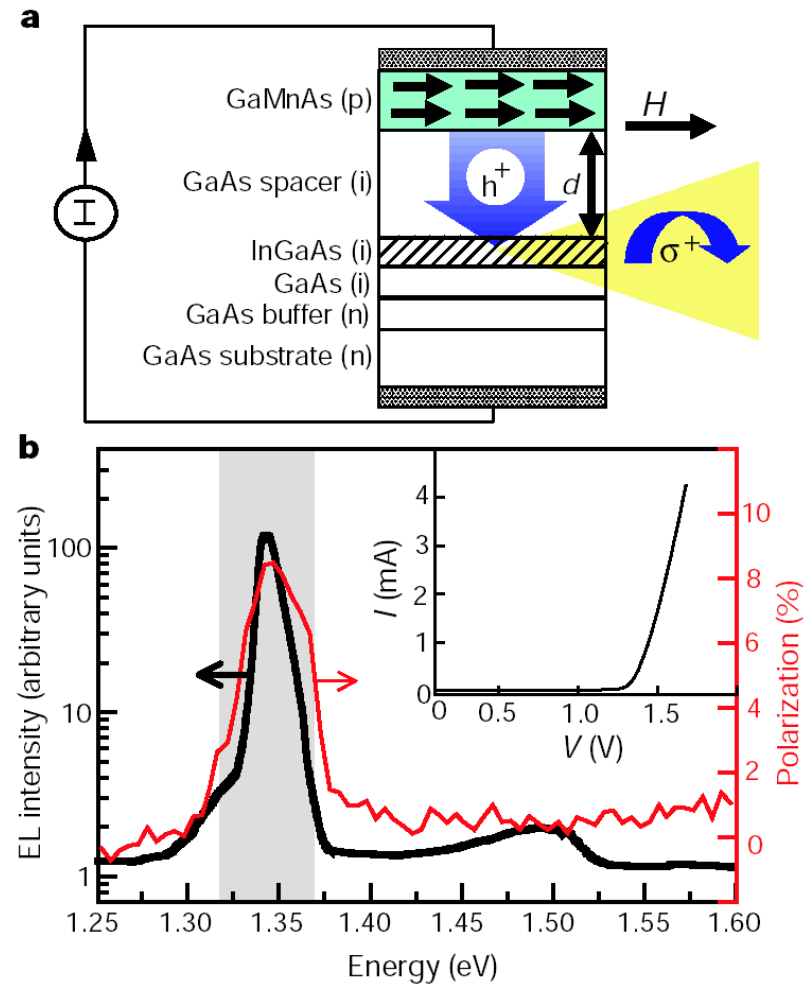


H. Ohno et al., JMMM, '99

Diluted magnetic semiconductors (DMS): Expected for future *spintronics* applications



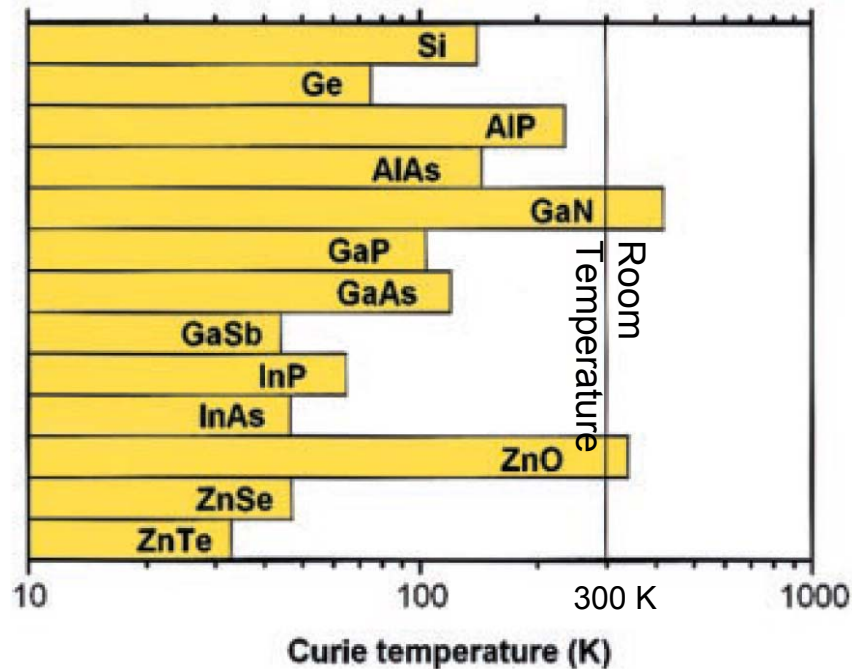
- GMR devices
- Non-volatile memories
- New logic circuits
- New devices utilizing spin injection
 - Circularly polarized LED
 - Magnetization control by spin current



Y. Ohno et al., Nature '99

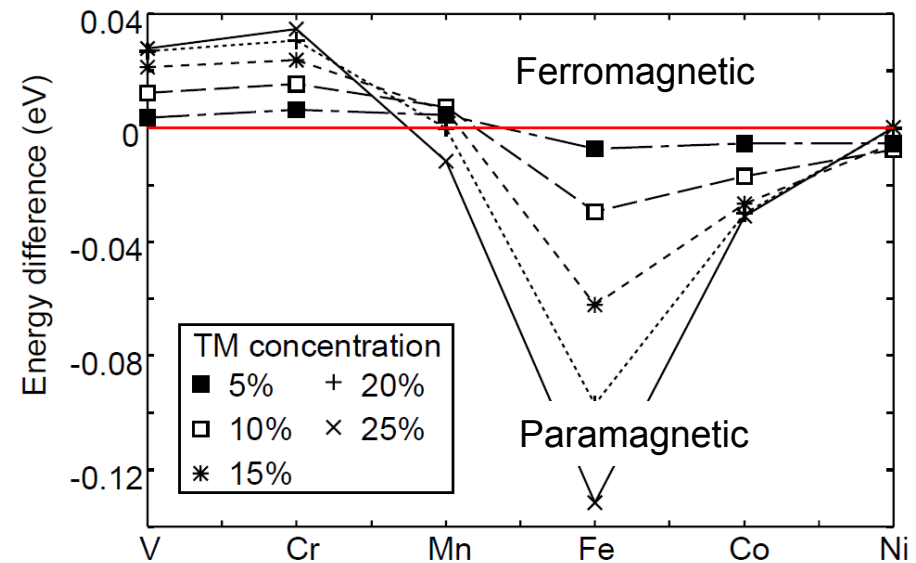
Theoretical prediction of room-temperature ferromagnetism in DMS

T_C of Mn-doped semiconductors in p - d exchange mechanism



T. Dietl et al. Science '00

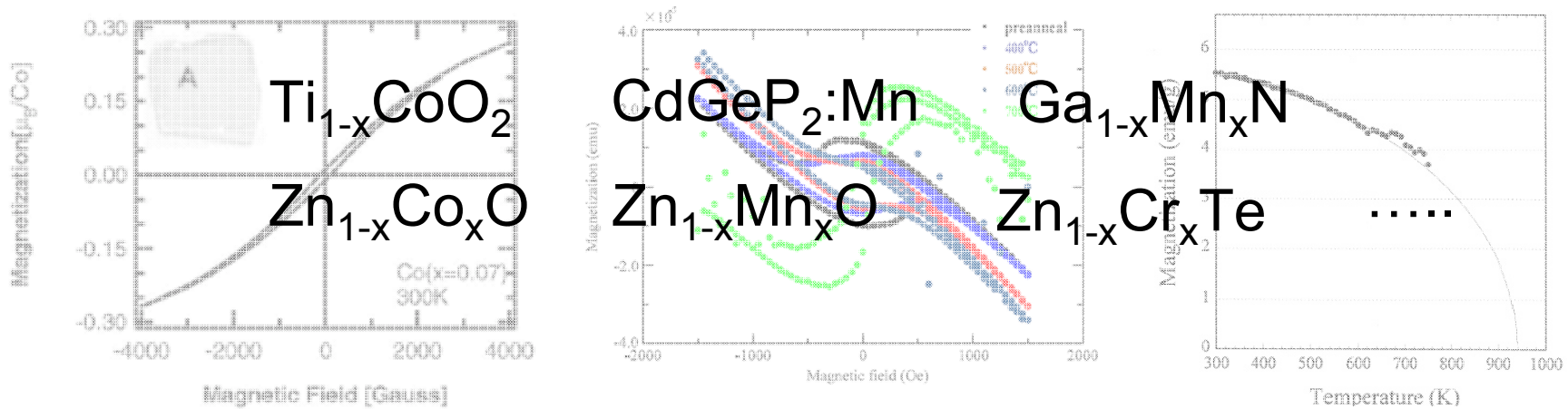
Stability of magnetic states in DMS in double-exchange mechanism



K. Sato et al. JJAP '00.

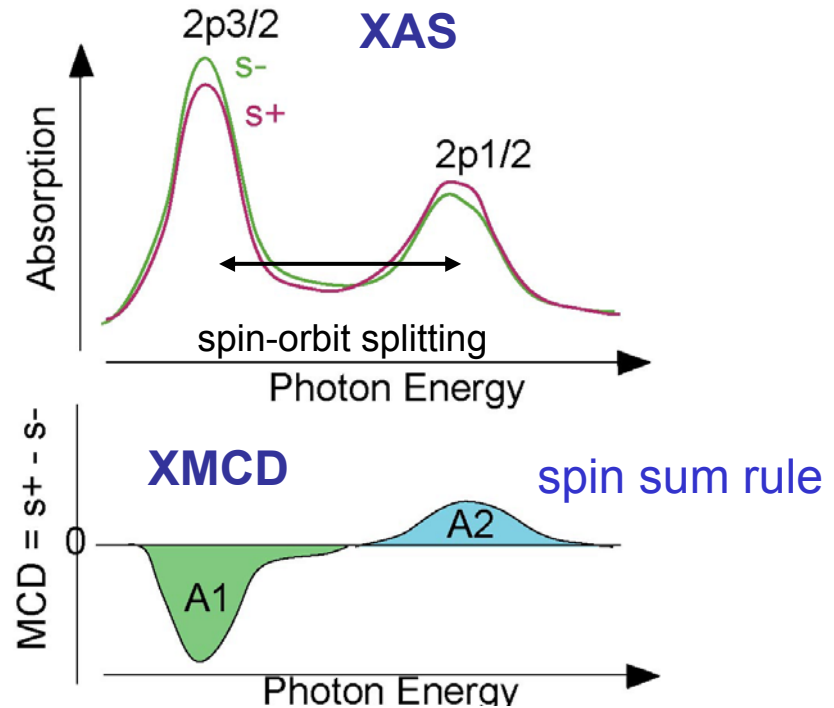
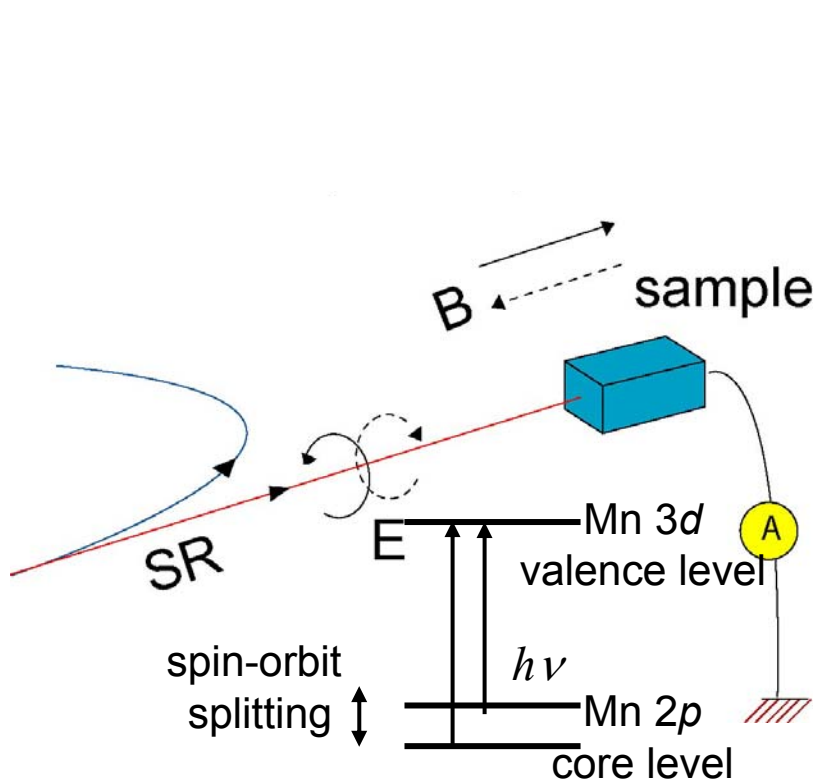
Wide-gap semiconductors such as ZnO, GaN, and TiO₂ are promising host materials for room-temperature ferromagnetic DMS.

Rom-temperature ferromagnetic DMS



- Are they intrinsic DMS?
 - No ferromagnetic contamination such as Fe metal?
 - No precipitation of second phases, etc?
- To answer these questions:
 - SQUID measurements are not sufficient
 - Anomalous Hall effect is useful but controversial

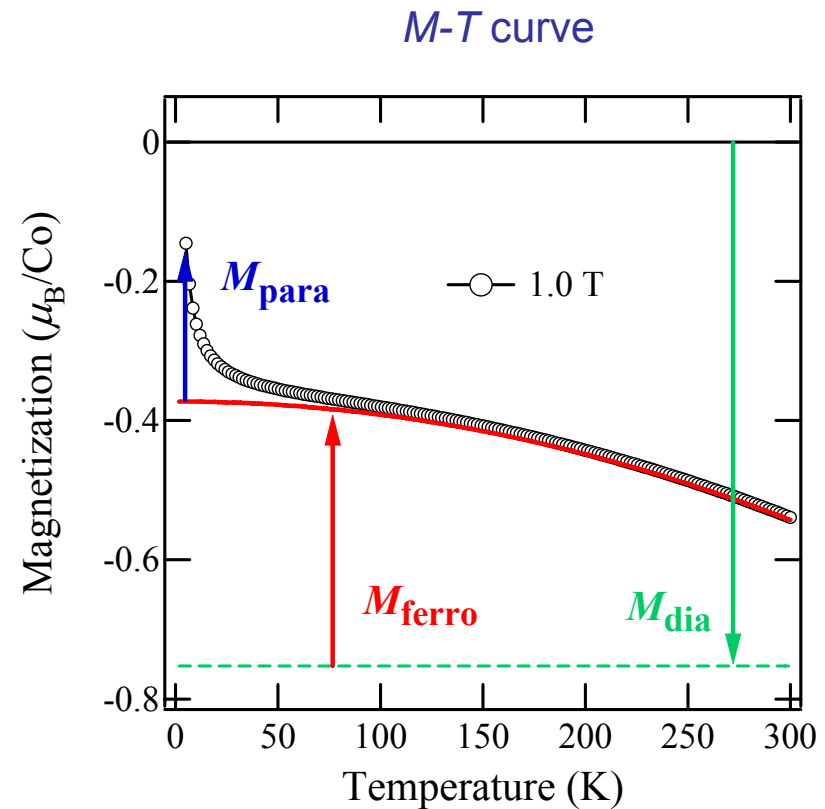
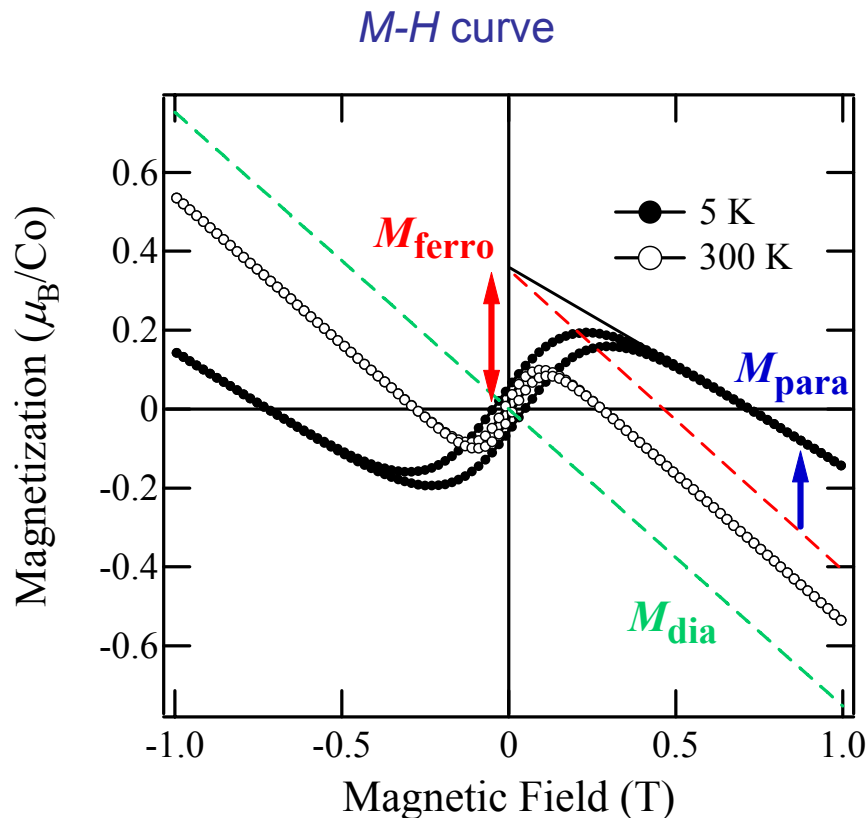
X-ray magnetic circular dichroism (XMCD) in core-level x-ray absorption spectra (XAS)



- Element-specific
- Chemical environment-specific
- Contamination-insensitive
- Magnetism-selective
- Drawback: Surface sensitivity

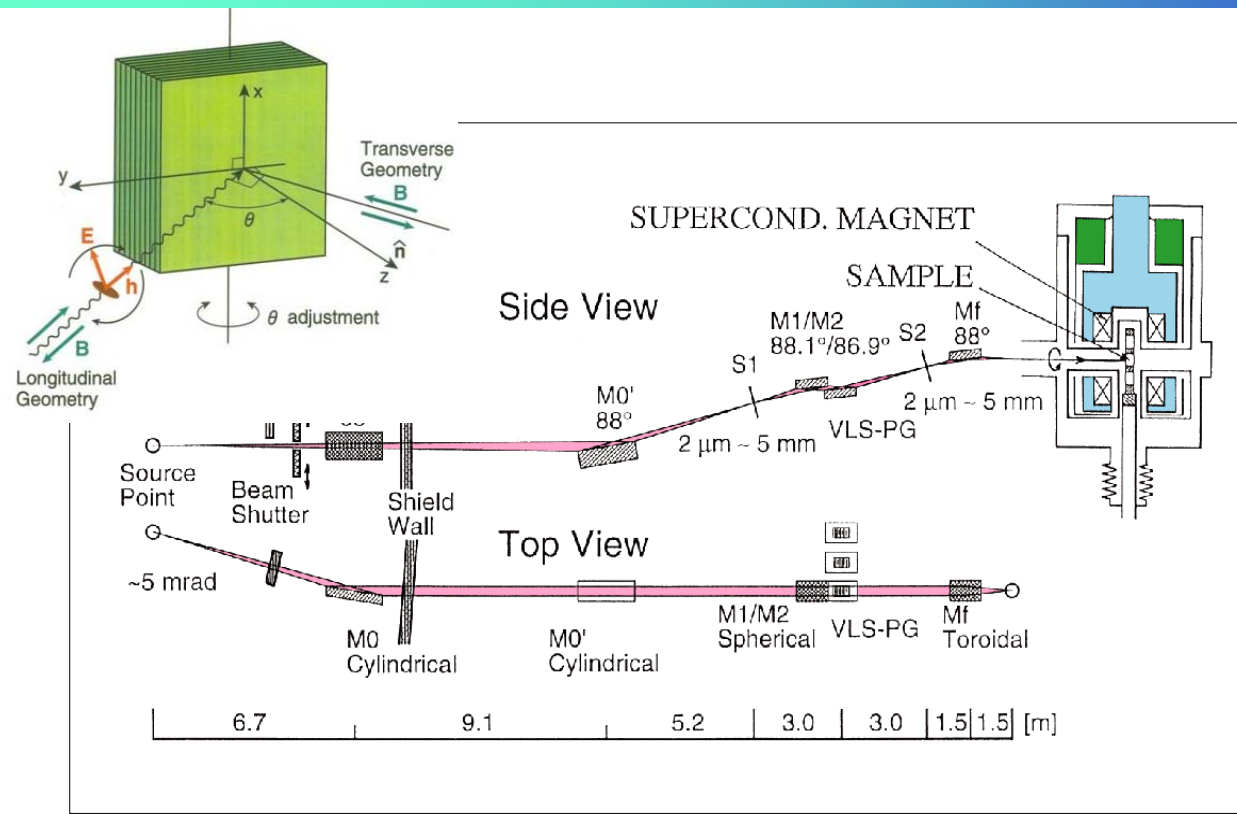
Ferromagnetic, paramagnetic and non-magnetic components in XMCD vs SQUID signals

SQUID data of a DMS thin film sample



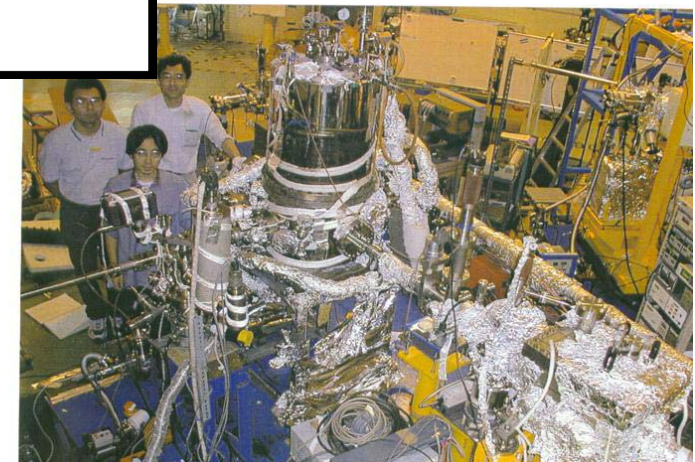
$$M = M_{\text{dia}} + \boxed{M_{\text{ferro}} + M_{\text{para}}} \rightarrow \text{XMCD signals, chemically decomposed}$$

XMCD experiment at BL11-A of Photon Factory (previous)



SC magnet $H < 5$ T
 $T > 10$ K
 Angle dependence

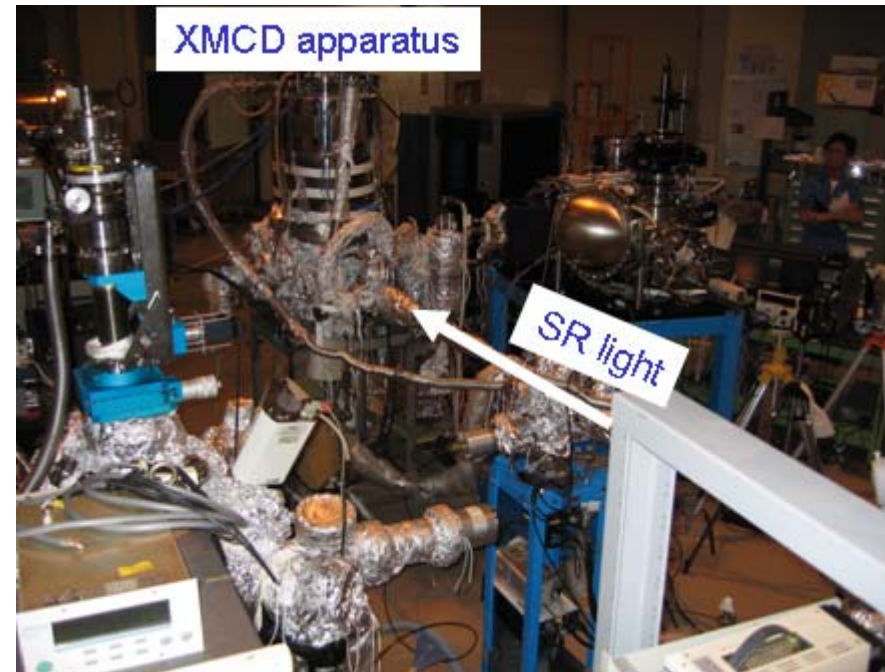
T. Koide et al. Rev. Rev. Sci. Instr. 63, 1462 (1992)



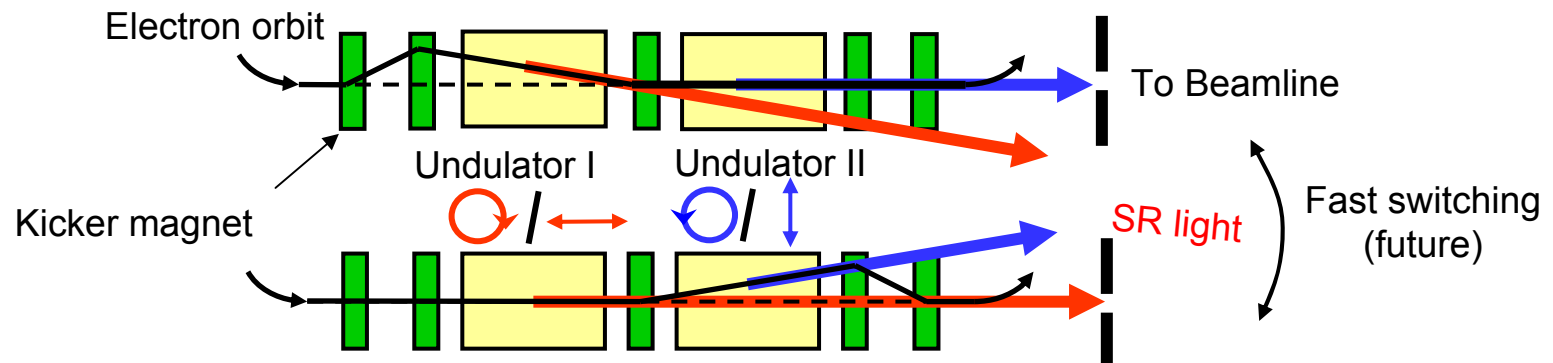
XMCD endstation at BL-16A of Photon Factory (present)



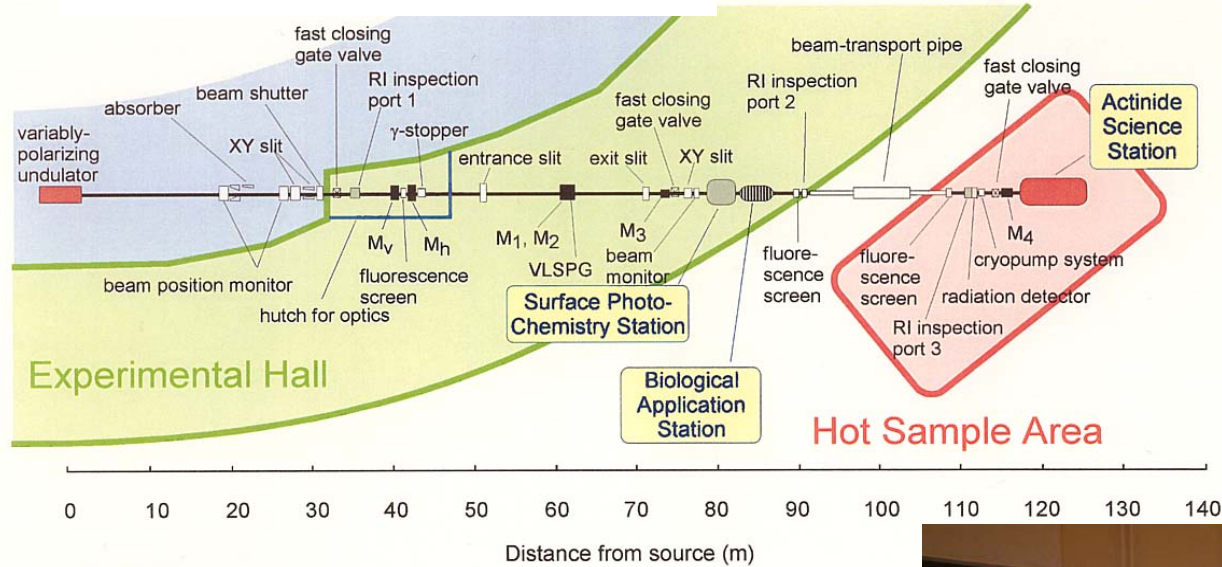
Superconducting magnet, up to 5 T
Low temperature down to ~10 K
Angular-dependent XMCD (L, T)



T. Koide et al. Rev. Rev. Sci. Instr. 63, 1462 (1992)



XMCD endstation at JAEA beamline BL-23SU of SPring-8



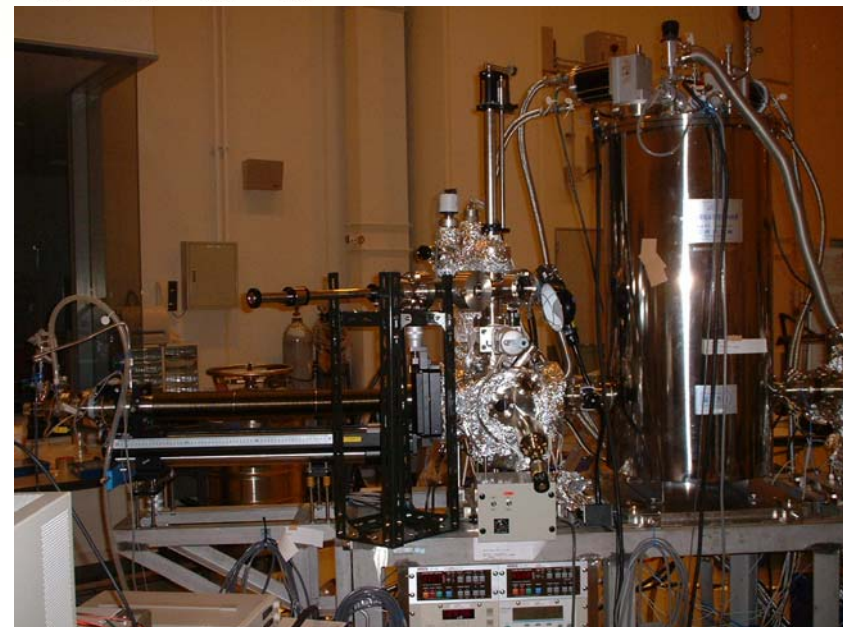
Helical undulator with phase modulation

Superconducting magnet, up to 10 T

Low temperature, down to ~6 K

High energy resolution and brightness monochromator

Y. Saitoh et al., Nucl. Instrum. Meth. A '01

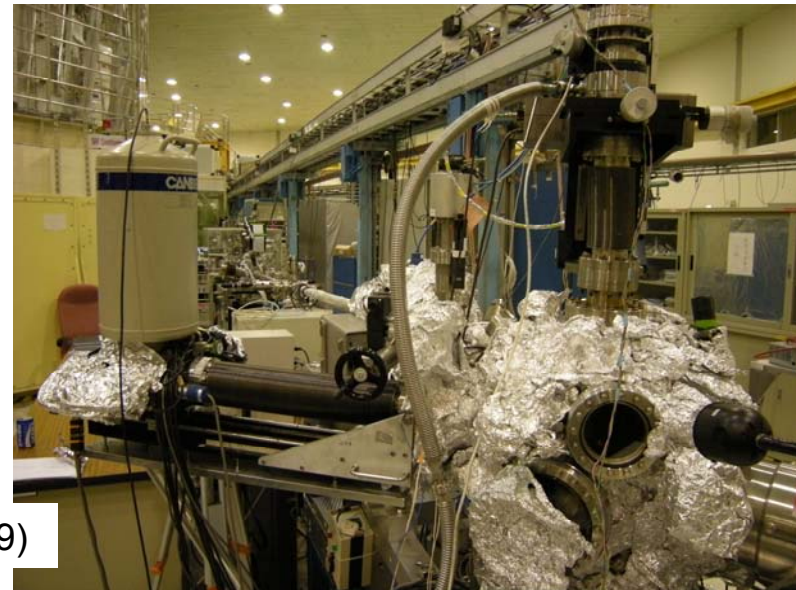


XMCD endstation at the Dragon beamline BL-11A at NSRRC

NSRRC, Taiwan

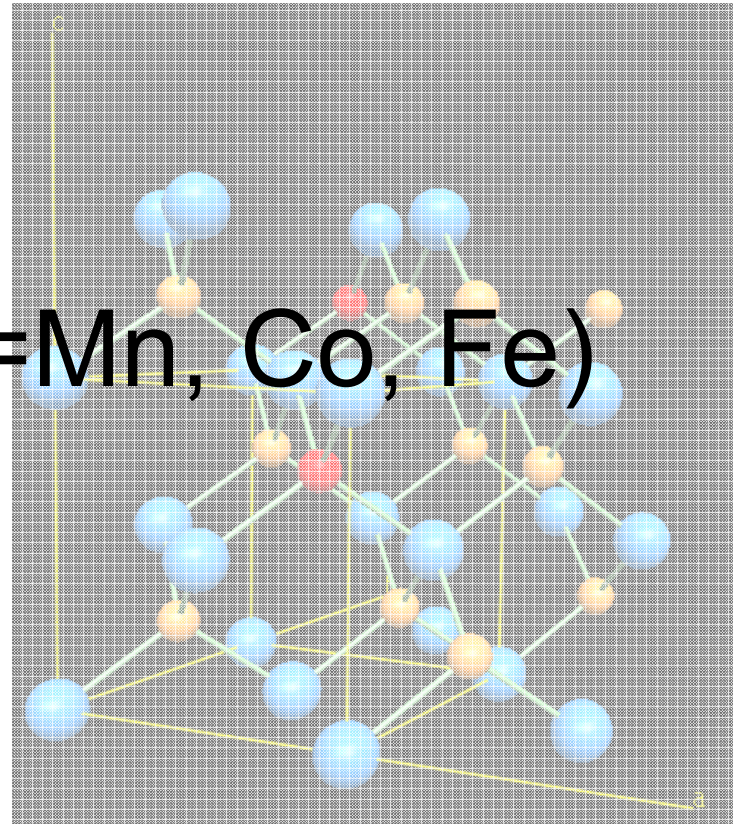
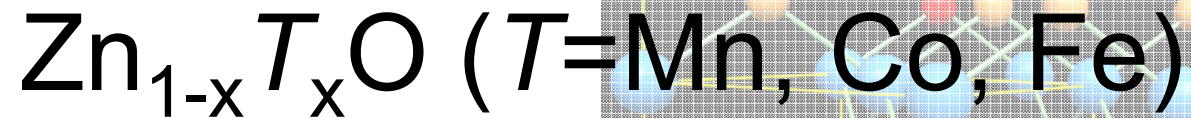


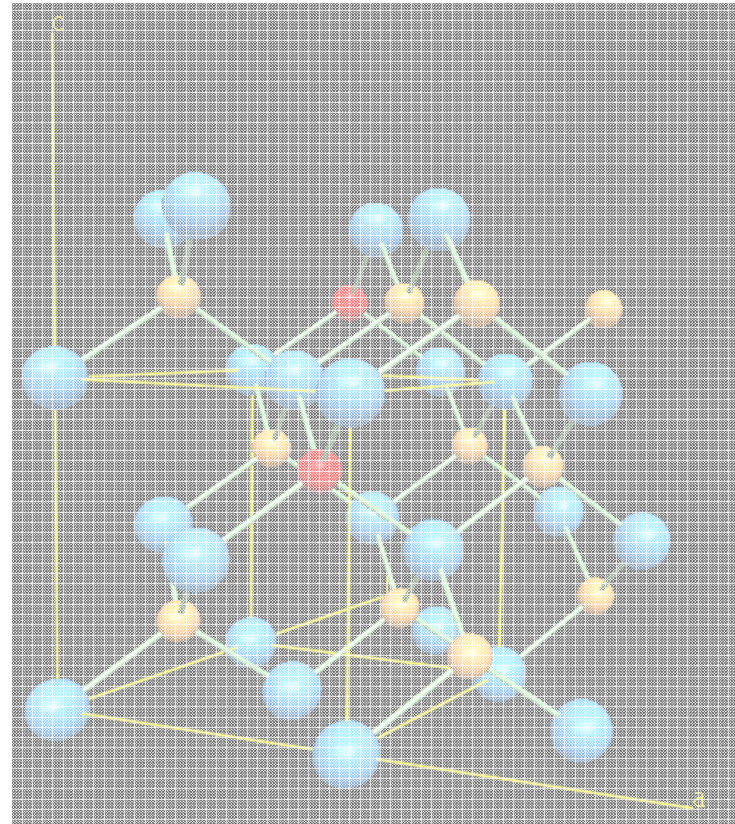
Bending magnet
Electro-magnet, up to 1 T
Low temperature down to 20 K
Total-electron-yield (TEY) and total-
fluorescence-yield (TFY) mode detections



C.T. Chen and F. Sette, Rev. Sci. Instr. 60, 1616 (1989)

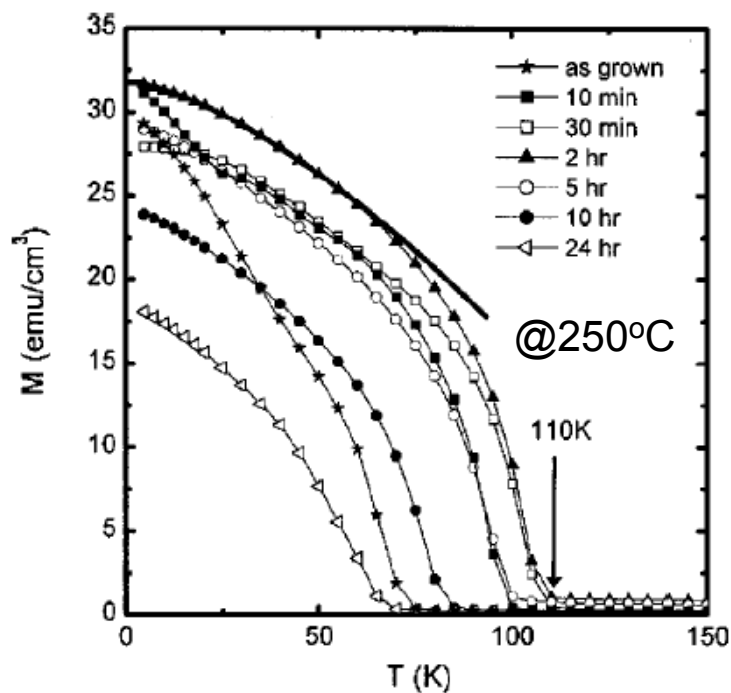
Outline





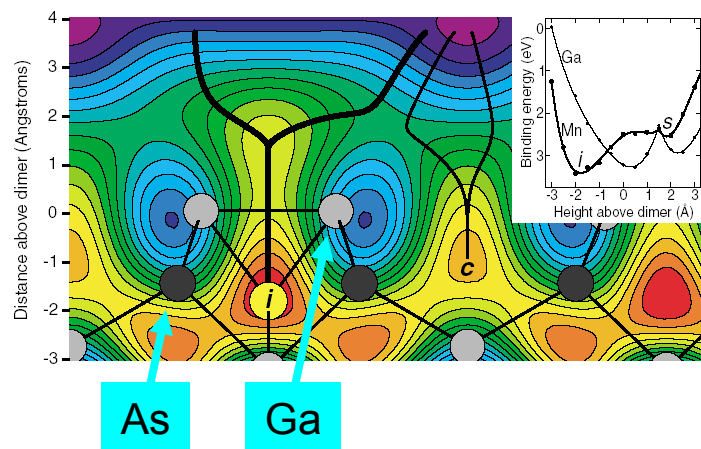
Effects of low-temperature post-annealing in $\text{Ga}_{1-x}\text{Mn}_x\text{As}$

Change of T_C by post-annealing



S.J. Potashnik et al., APL '01
T. Hayashi et al., APL '01

Molecular dynamic calculation

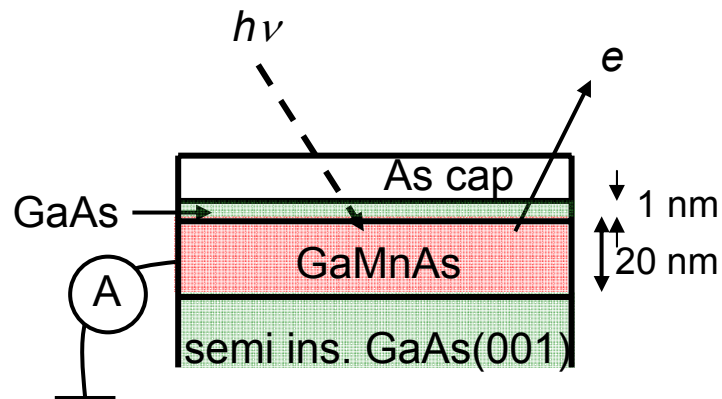


Mn first enters **interstices** then substitutes Ga.

S.C. Erwin and A.G. Petukhov PRL '02

Ga_{1-x}Mn_xAs samples

Sample: as grown Ga_{1-x}Mn_xAs



As-grown: $x = 0.042, 0.078$

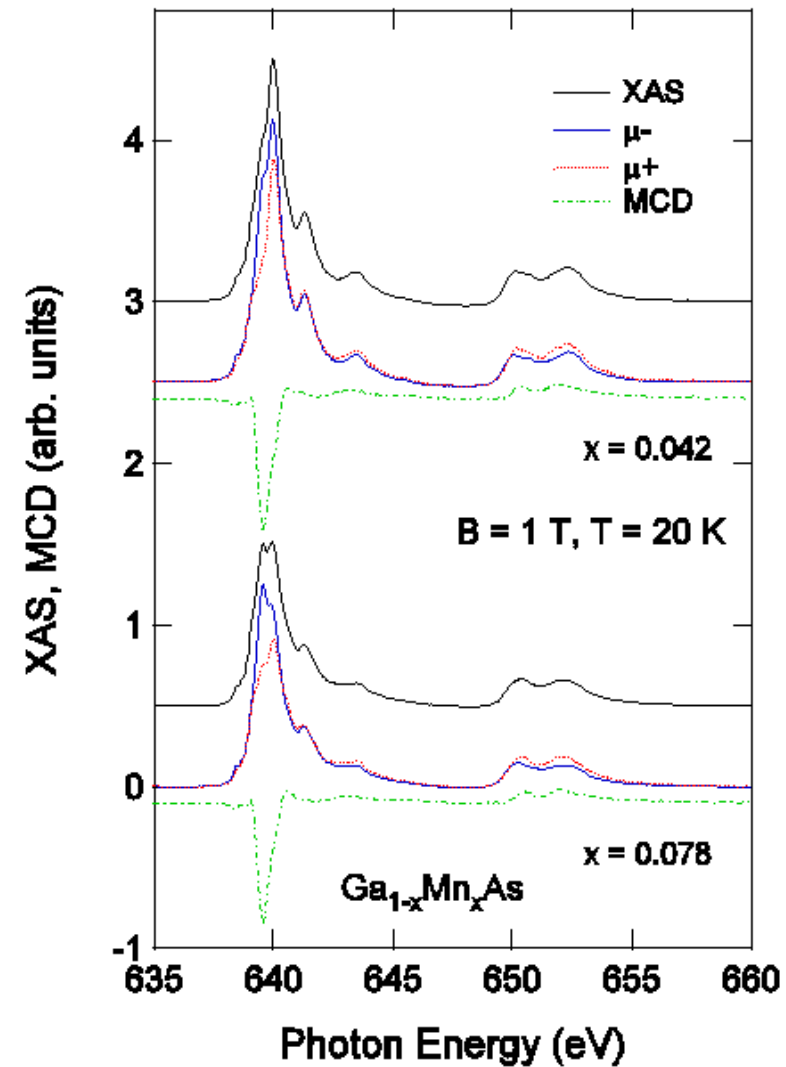
$T_C \sim 60$ K

Post-annealed: $x = 0.04$, @270°C, 2 h

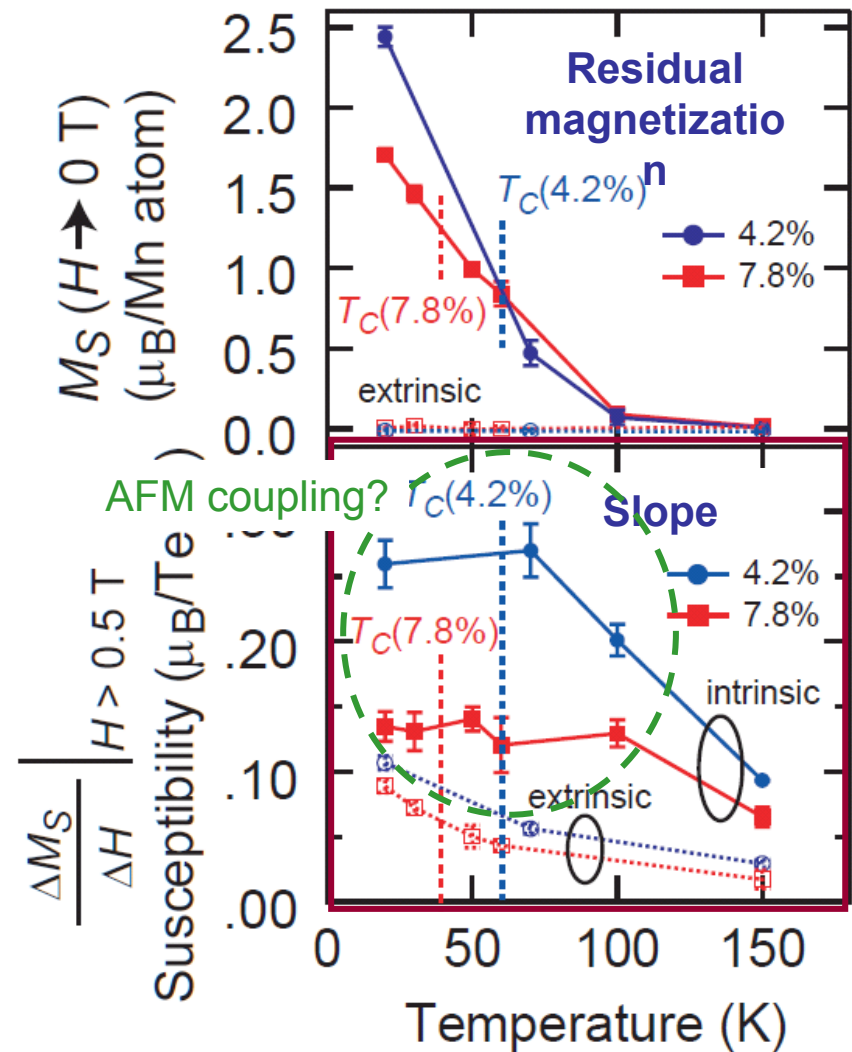
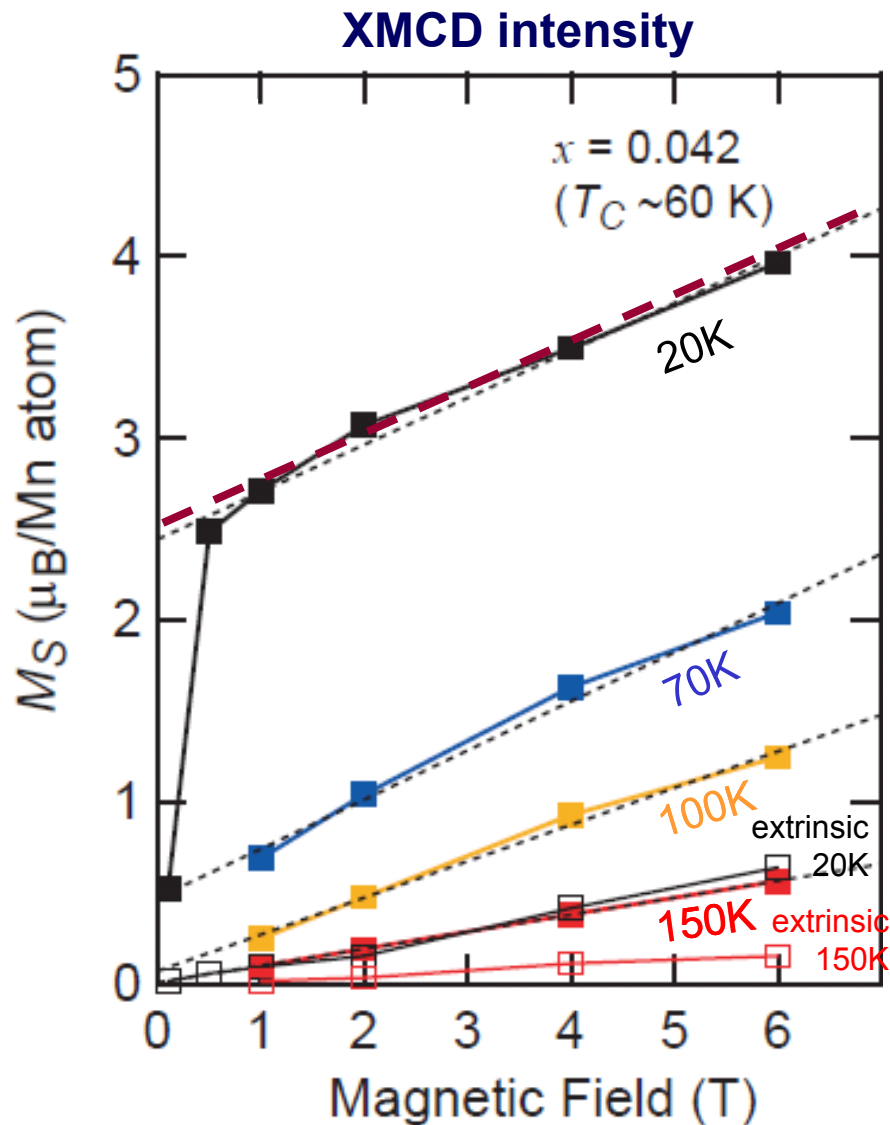
$T_C \sim 120$ K

SPring-8 BL23SU

XAS and XMCD spectra

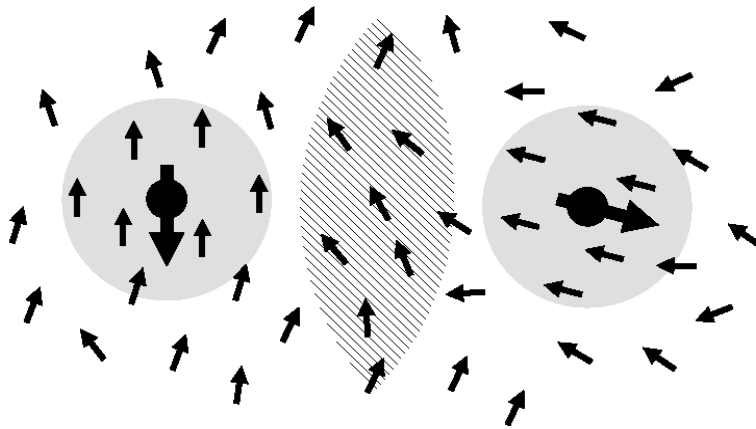


Paramagnetic component of XMCD vs T in as-grown $\text{Ga}_{1-x}\text{Mn}_x\text{As}$

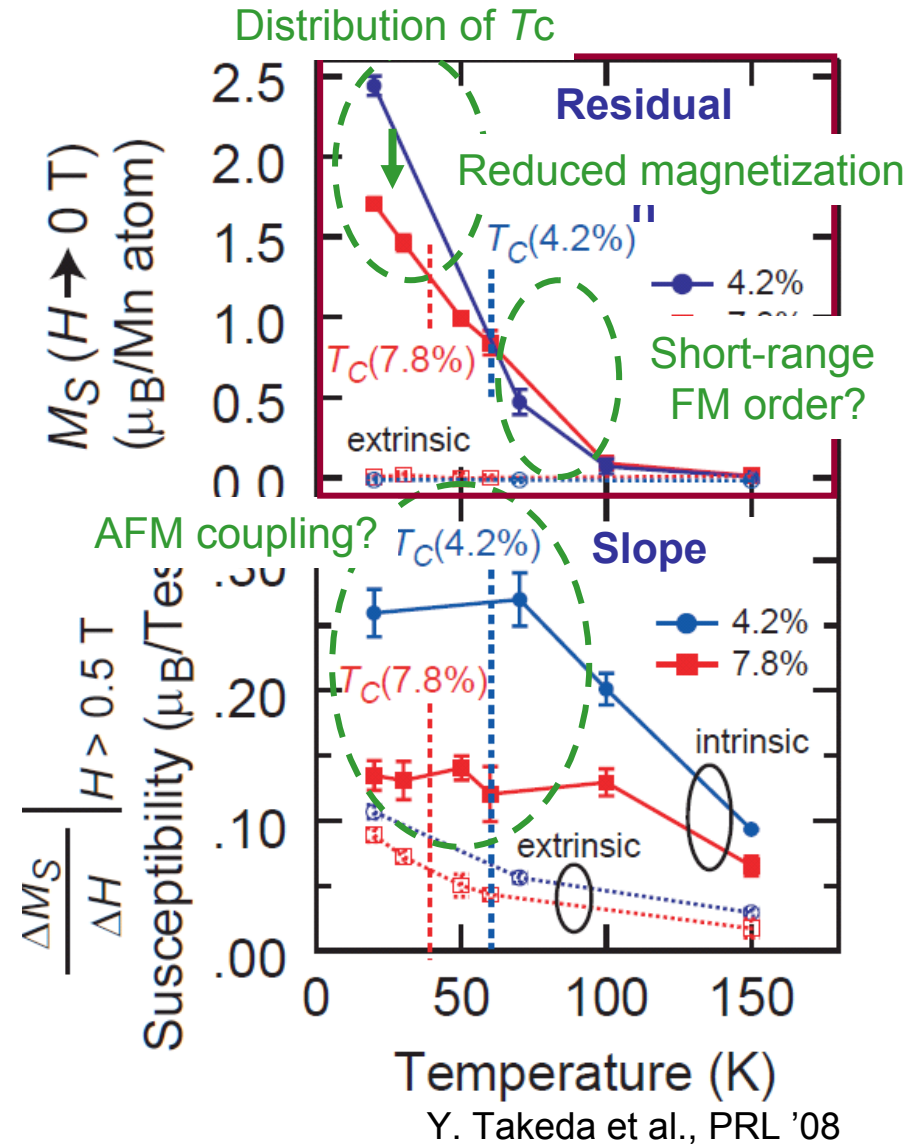


Ferromagnetic component of XMCD vs T in as-grown $\text{Ga}_{1-x}\text{Mn}_x\text{As}$

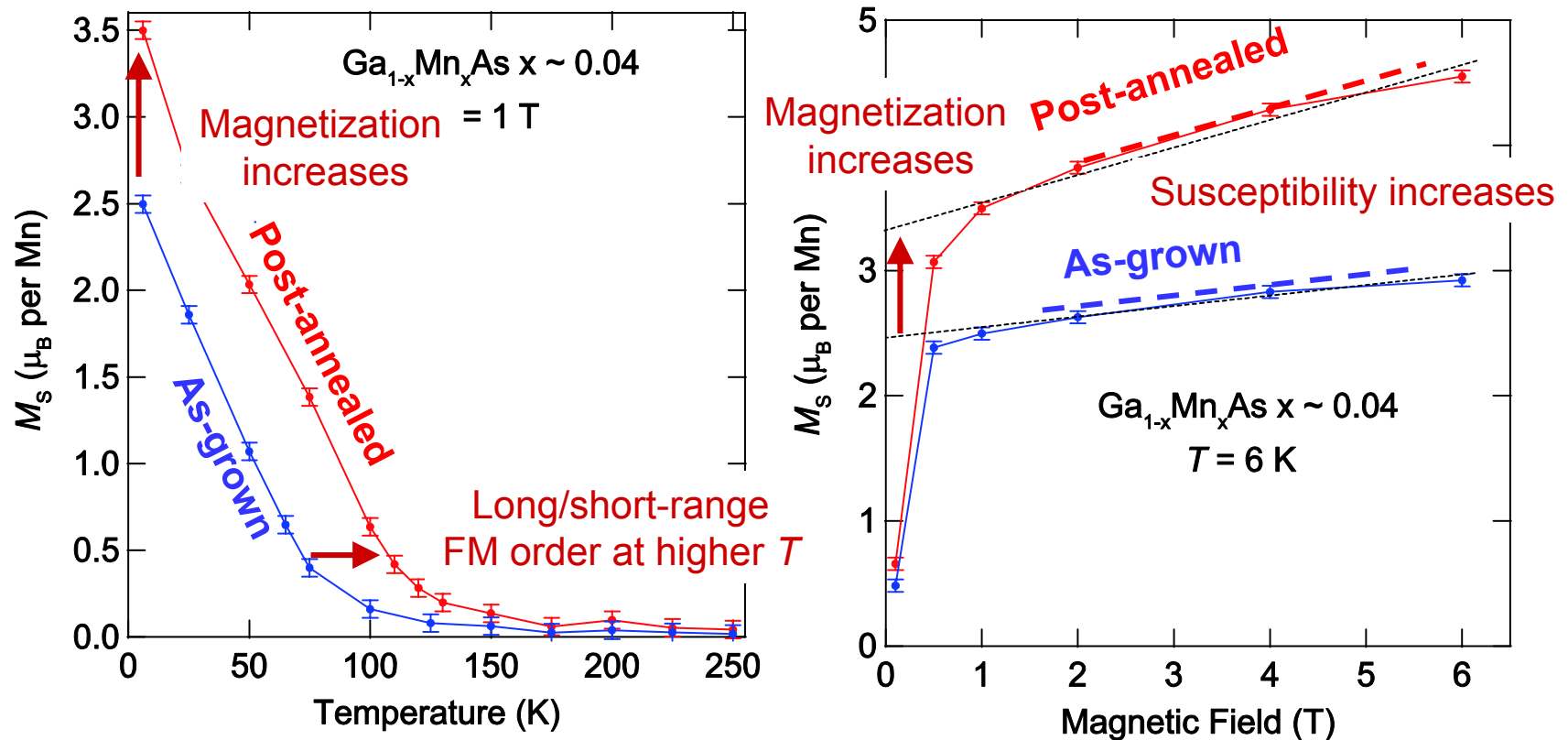
Magnetic polarons?



A. Kaminski and S. Das Sarma, PRL '02

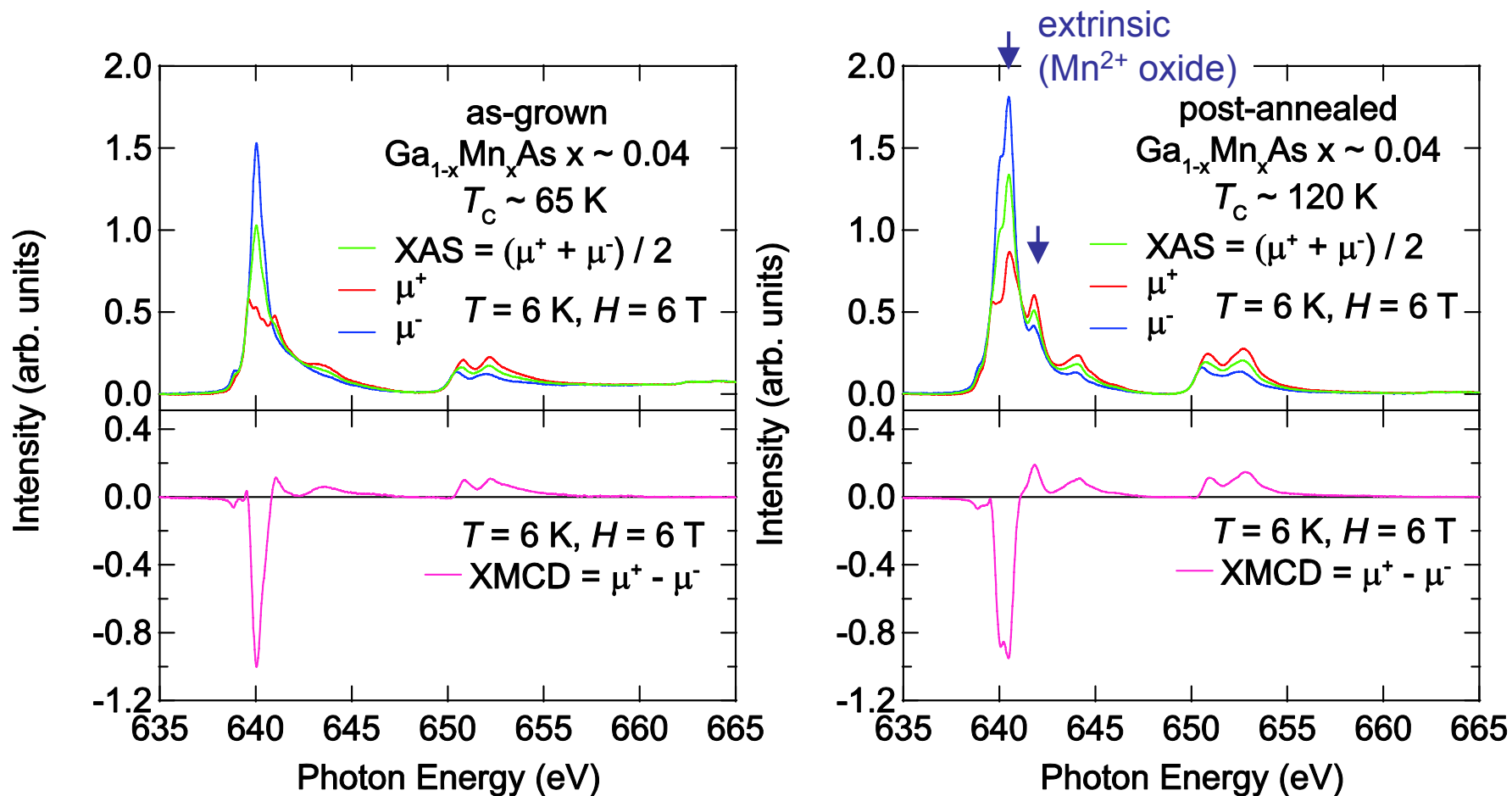


Effects of post annealing on XMCD intensities vs T & H in $\text{Ga}_{1-x}\text{Mn}_x\text{As}$

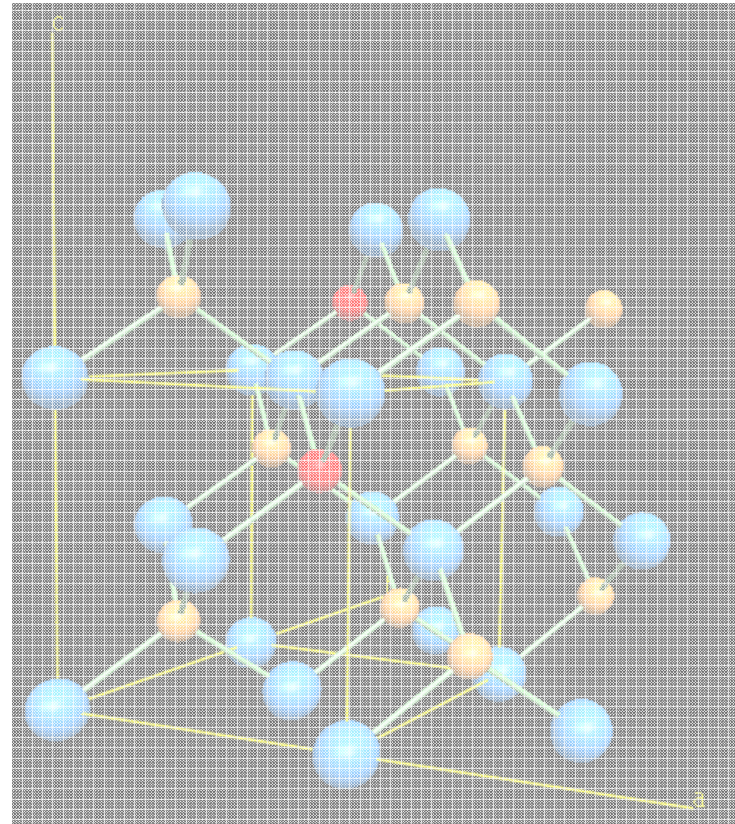


Post annealing diminishes AF interaction by reducing the number of *interstitial* Mn ions.

Effects of low-temperature post-annealing on XAS and XMCD of $\text{Ga}_{1-x}\text{Mn}_x\text{As}$

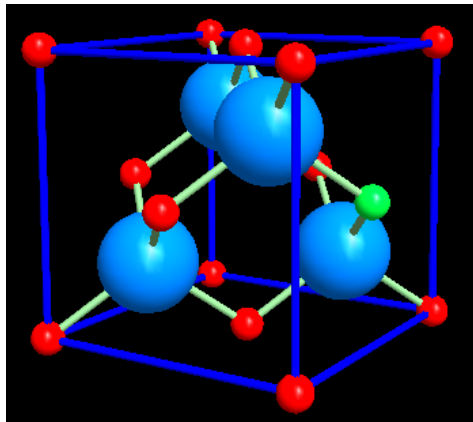
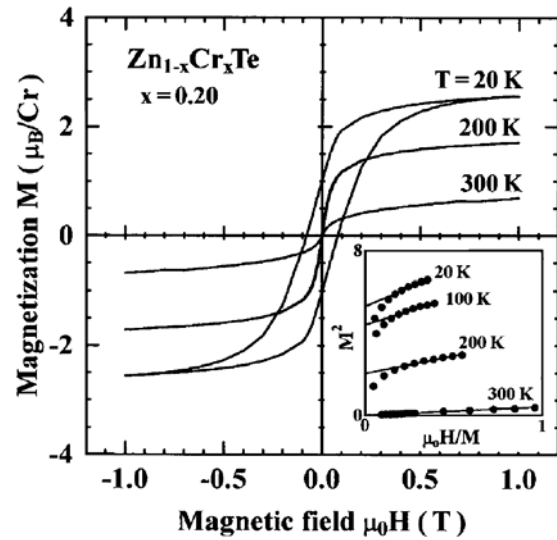


Post annealing expels *interstitial* Mn ions to surface

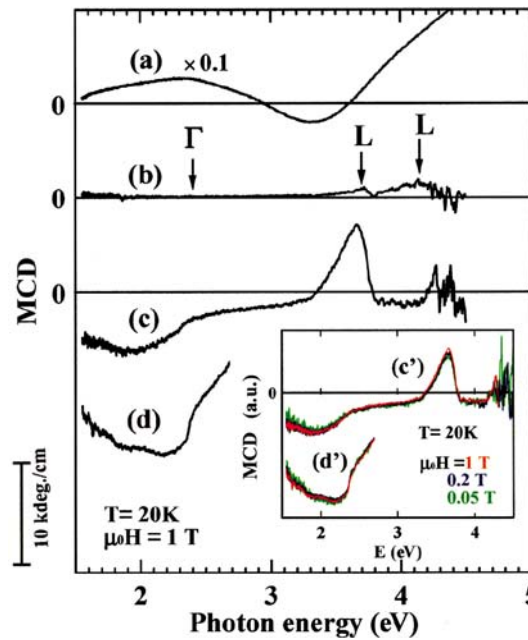


Diluted ferromagnetic semiconductor $Zn_{1-x}Cr_xTe$

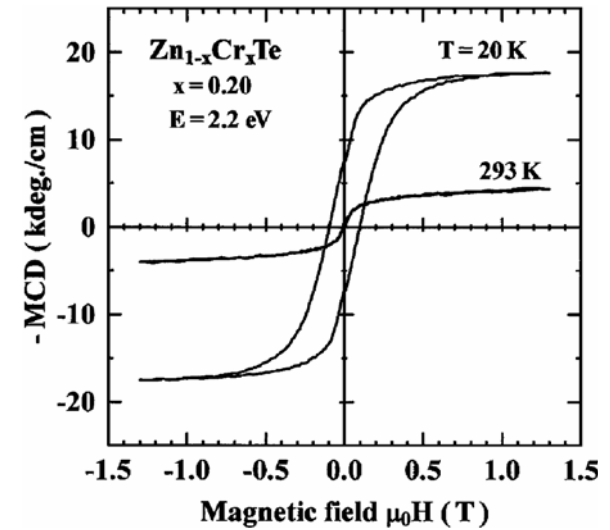
M-H curves



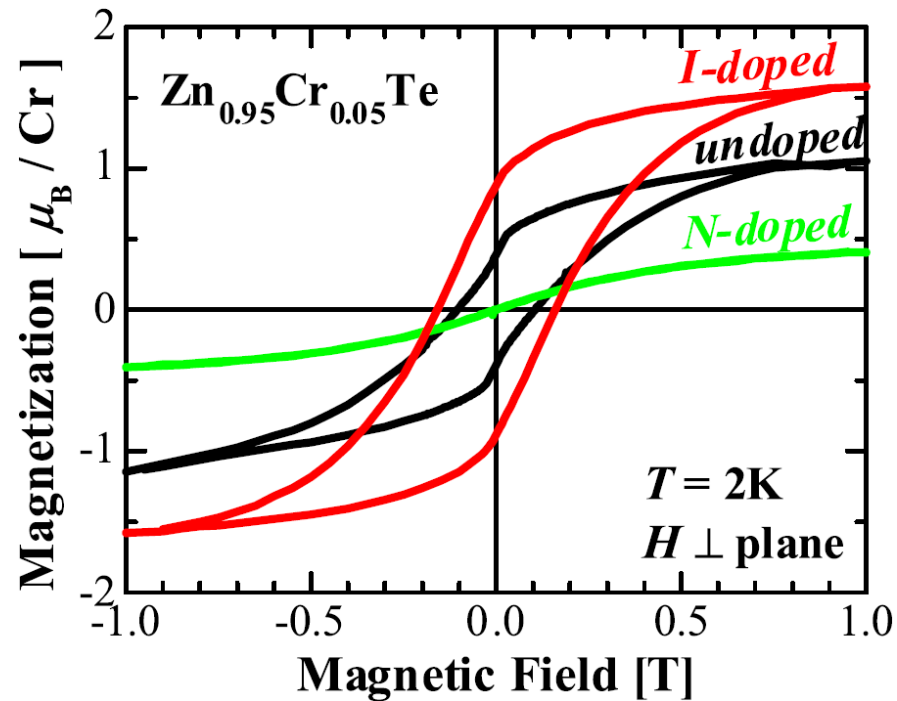
VIS-UV MCD



MCD vs H

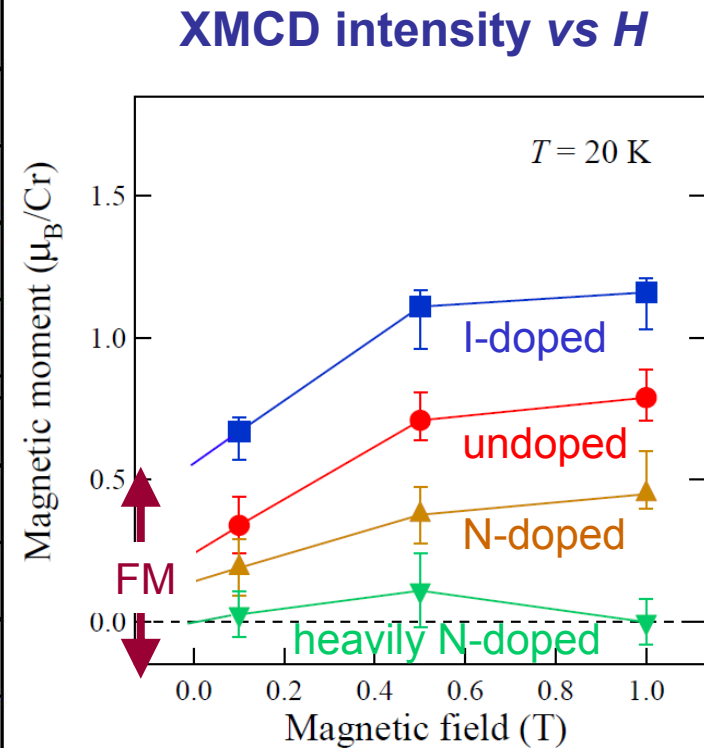
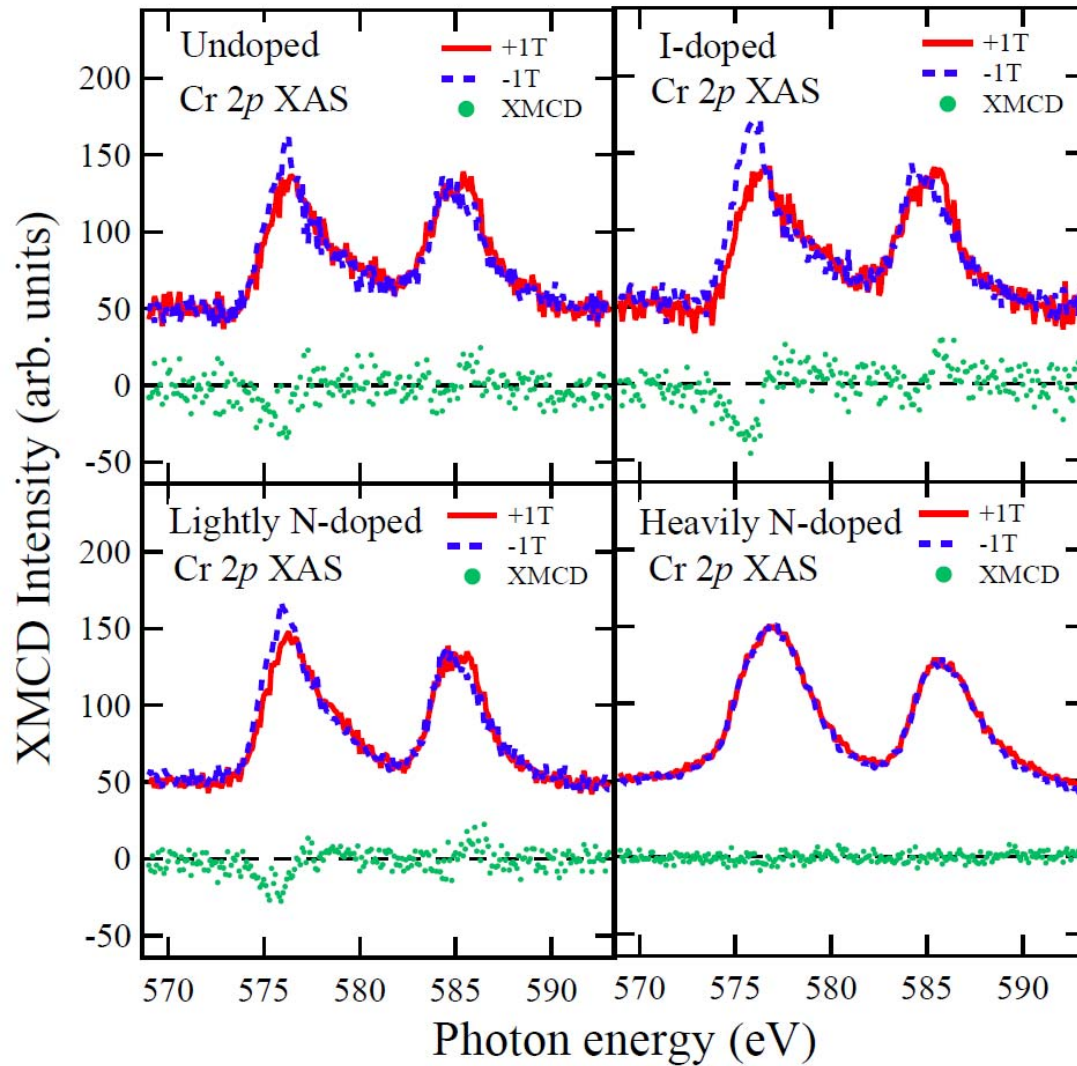


Doping effects in $\text{Zn}_{1-x}\text{Cr}_x\text{Te}$



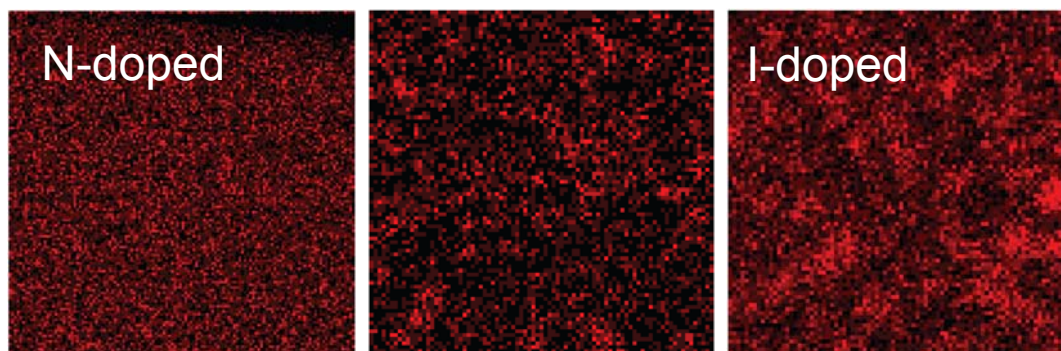
I-doping: Electron-doped
N-doping: Hole-doped

Doping effects in $\text{Zn}_{1-x}\text{Cr}_x\text{Te}$: XMCD



Inhomogeneous distribution of Cr in $\text{Zn}_{1-x}\text{Cr}_x\text{Te}$

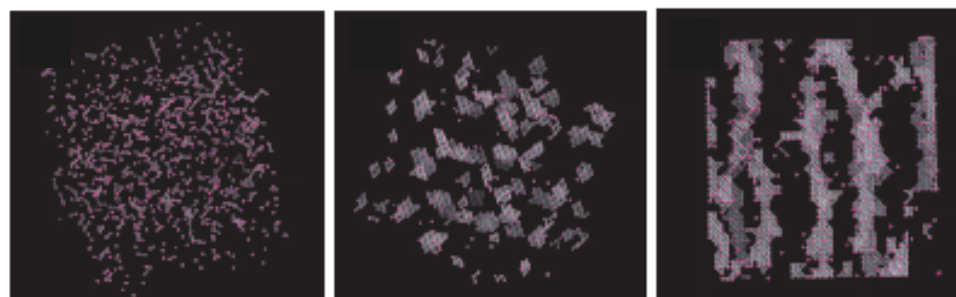
Energy-dispersive X-ray spectroscopy image



uniform T_C low \longleftrightarrow non-uniform T_C high

S. Kuroda et al., Nat. Mater. '07

Spinodal decomposition in high- T_C DMS's

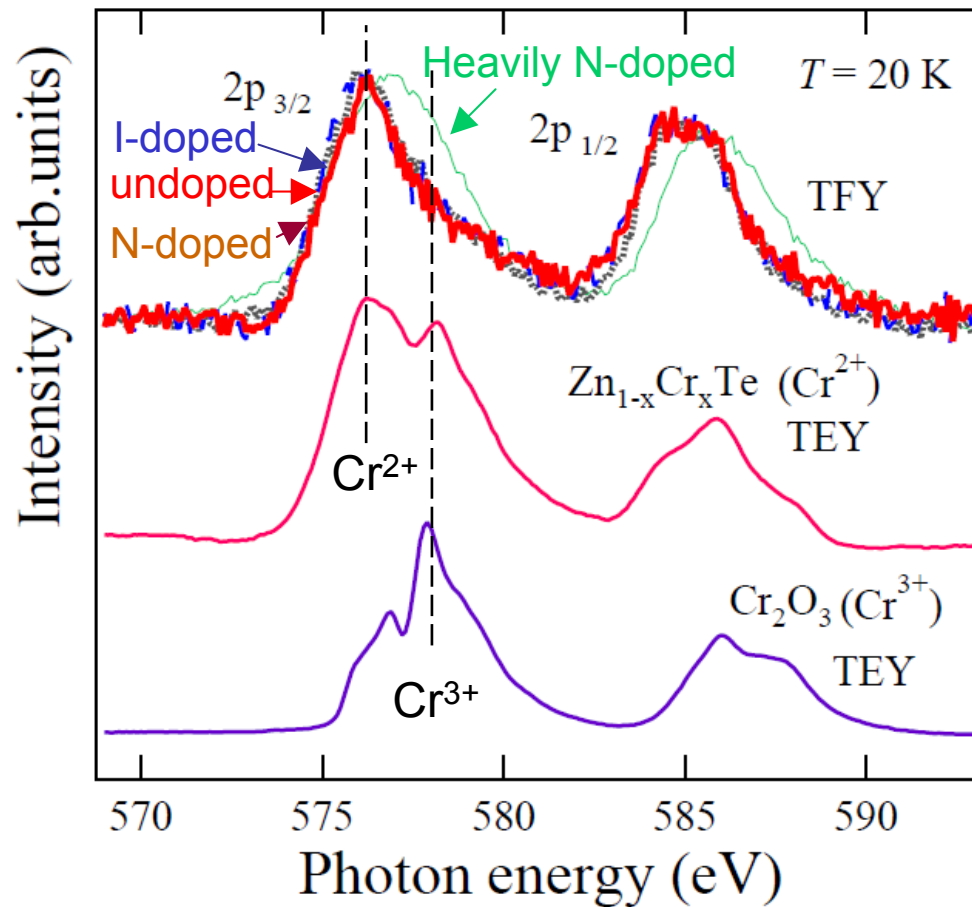


K. Sato et al., JJAP '05

T. Fukushima et al., JJAP '06

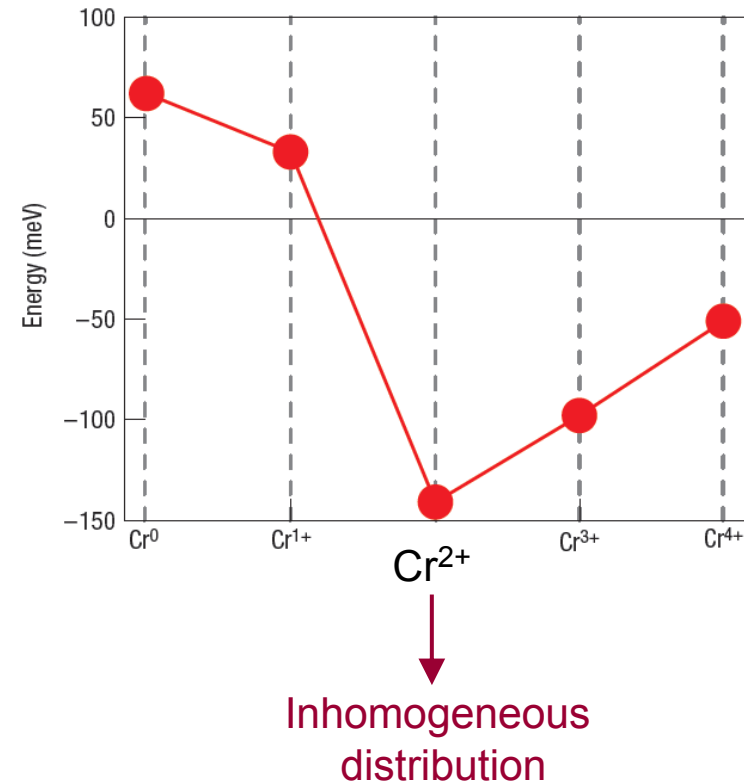
Cr valence vs inhomogeneous distribution of Cr in $Zn_{1-x}Cr_xTe$

Cr 2p XAS of $Zn_{1-x}Cr_xTe$

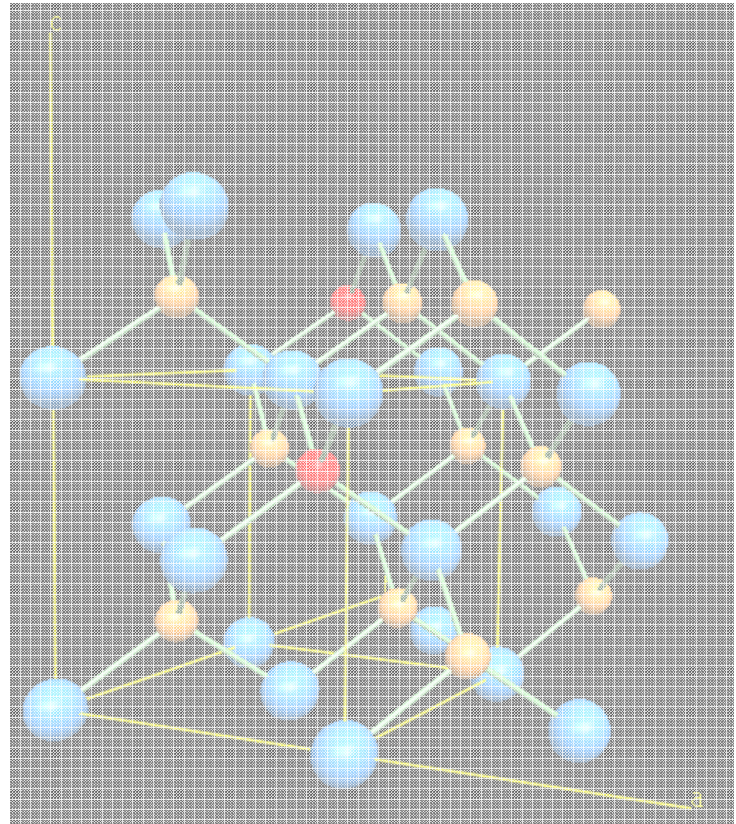
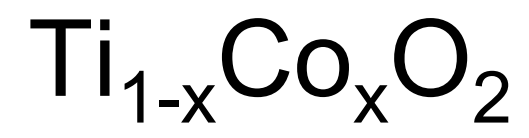


Y. Yamazaki et al.

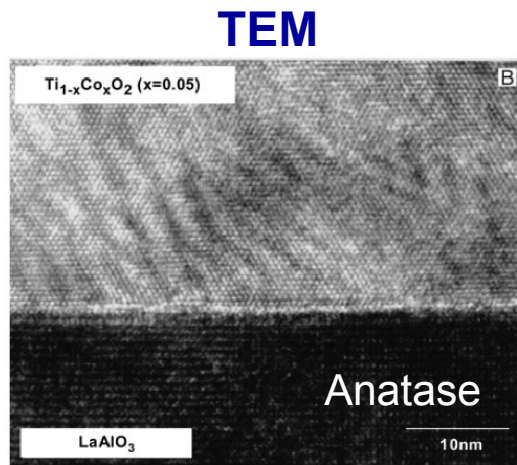
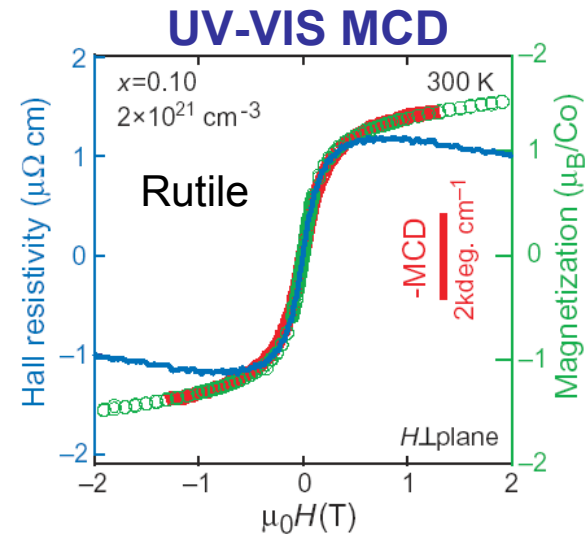
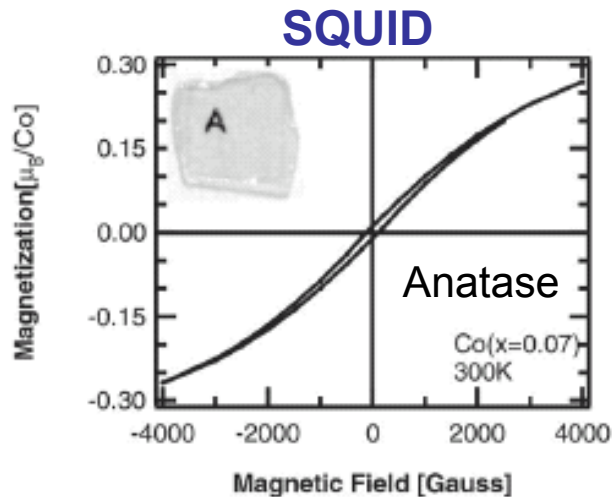
Cr-Cr pair formation energy



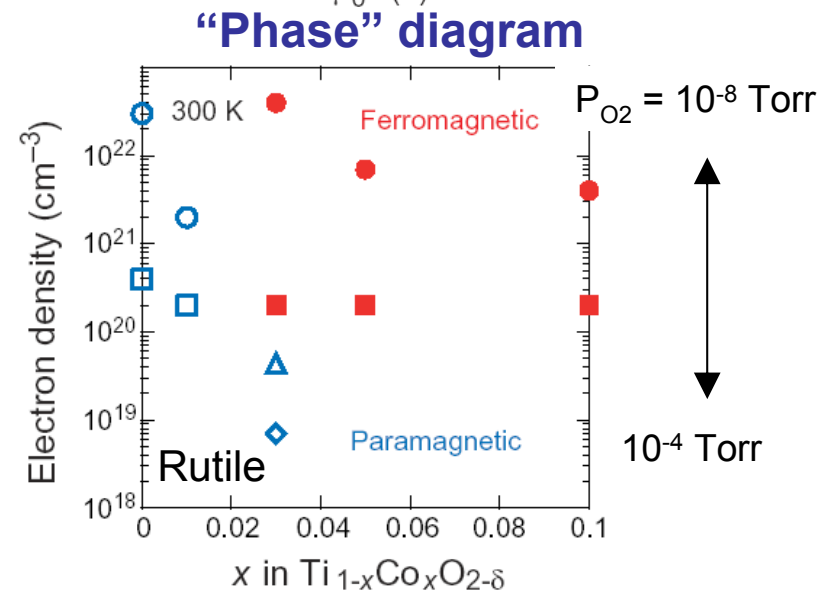
S. Kuroda, T. Dietl et al., Nat. Mater. '07



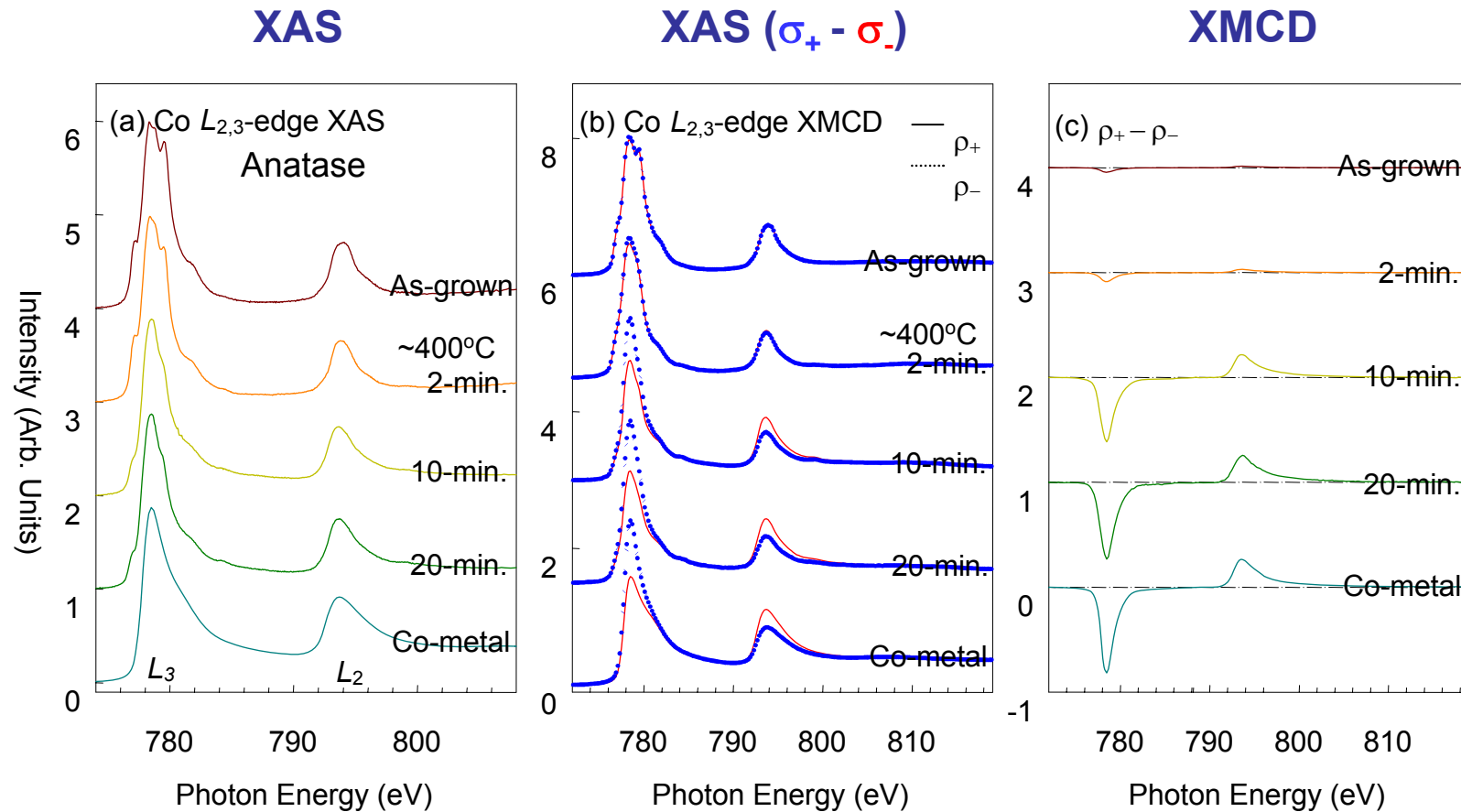
Room-temperature ferromagnetism in $\text{Ti}_{1-x}\text{Co}_x\text{O}_2$



No precipitation

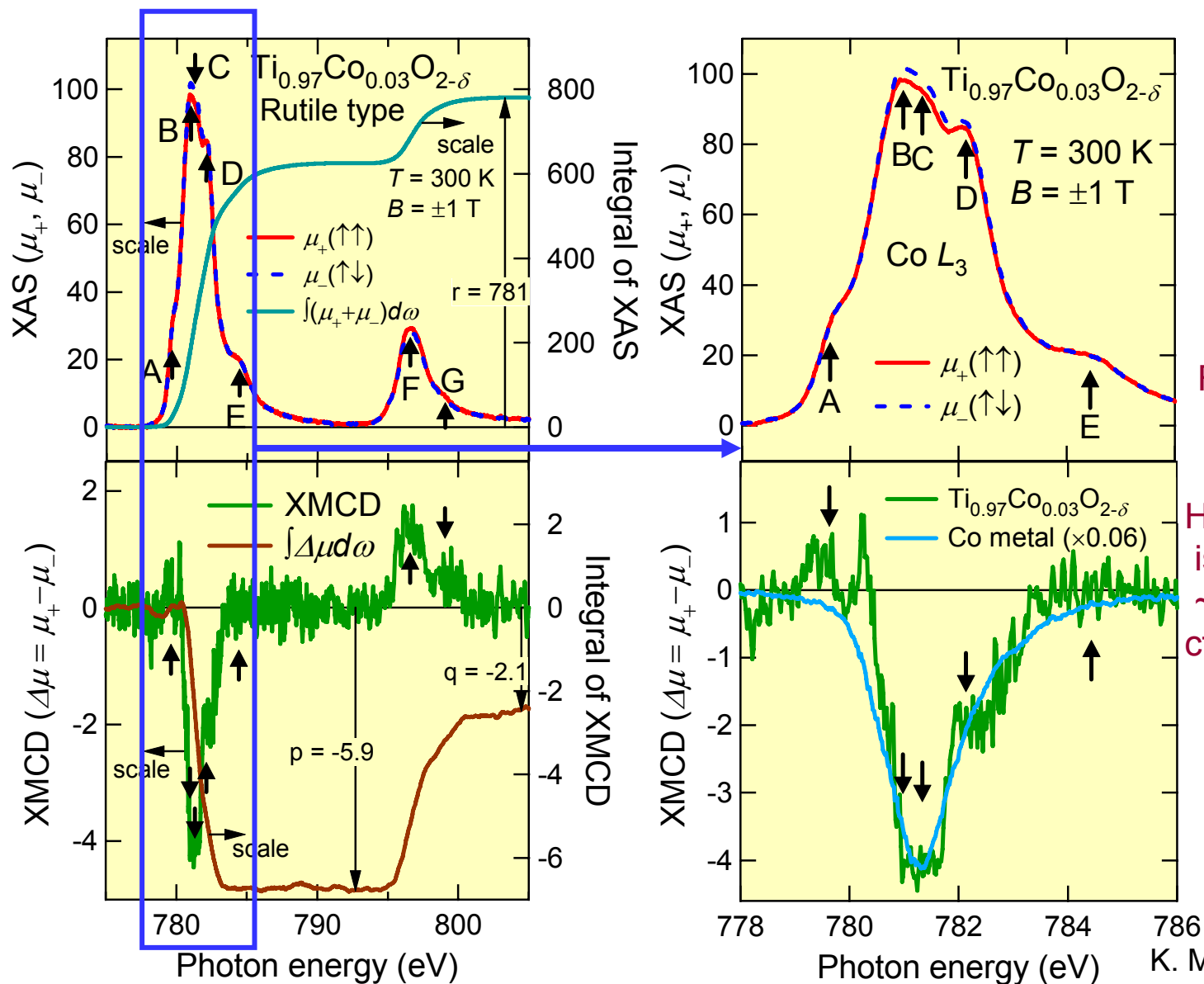


Co 2p core-level XAS and XMCD of $Ti_{1-x}Co_xO_2$: Effect of high- T annealing in vacuum



“Ferromagnetism is due to segregated Co metal.”

Co 2p core-level XMCD of $\text{Ti}_{1-x}\text{Co}_x\text{O}_2$ without high- T annealing



Ferromagnetism is due to Co^{2+} ion

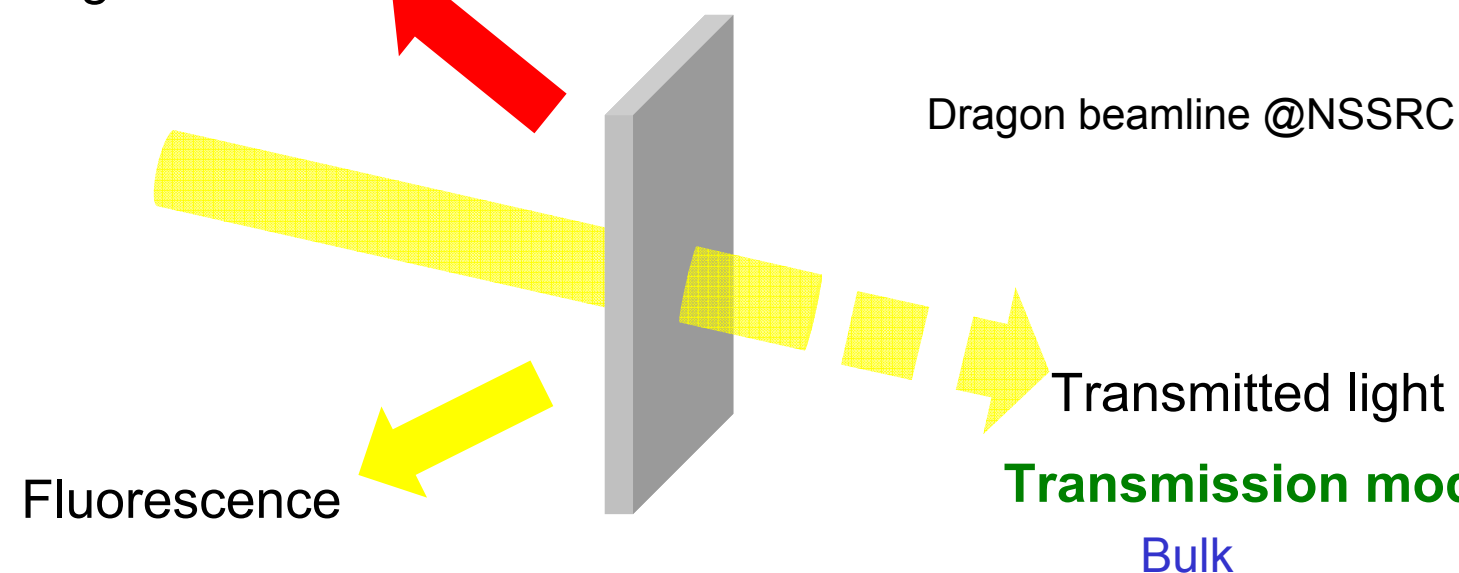
However, moment is very small:
 $\sim 0.13 \mu_B/\text{Co}$
 cf. SQUID $\sim 1 \mu_B/\text{Co}$

Surface- and bulk-sensitive modes of XAS and XMCD measurements

Total electron yield (TEY) mode

probing depth ~ 3-5nm

Auger electron

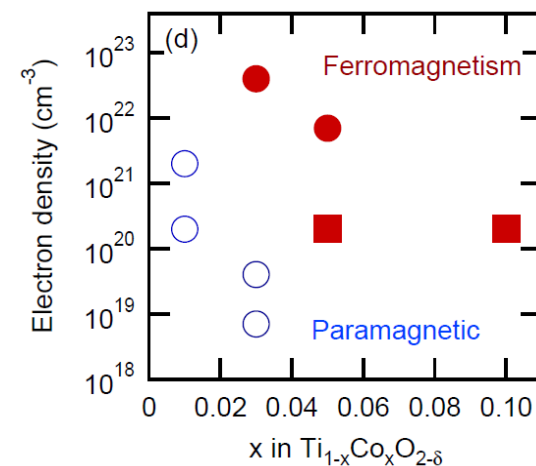
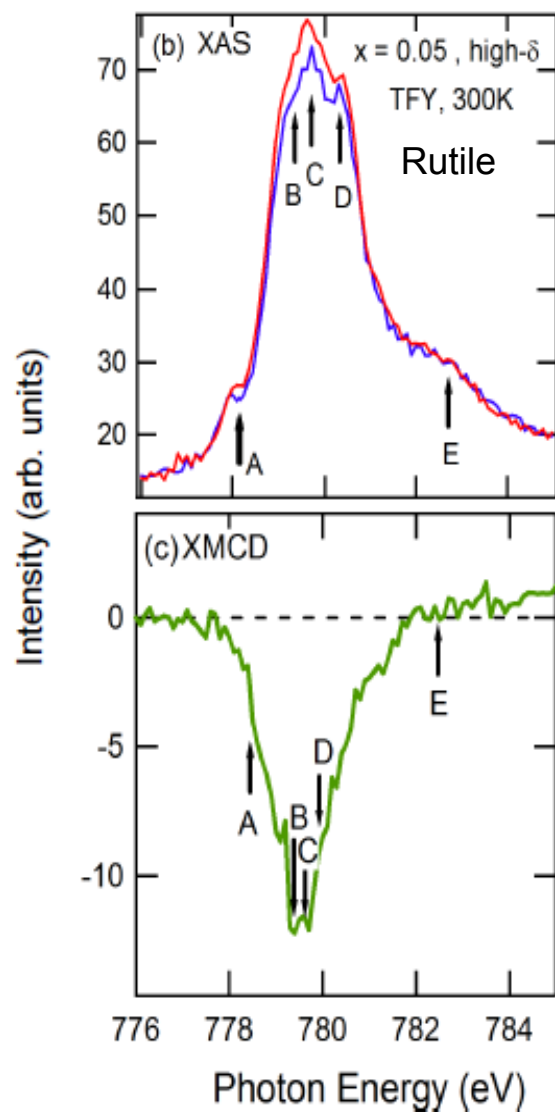
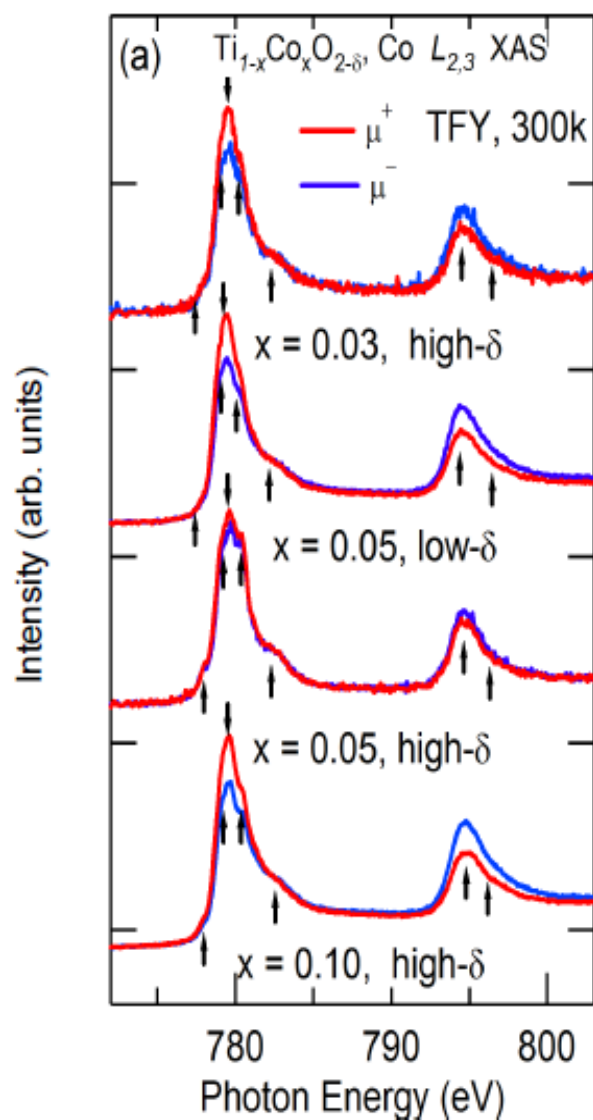


Total fluorescence yield (TFY) mode

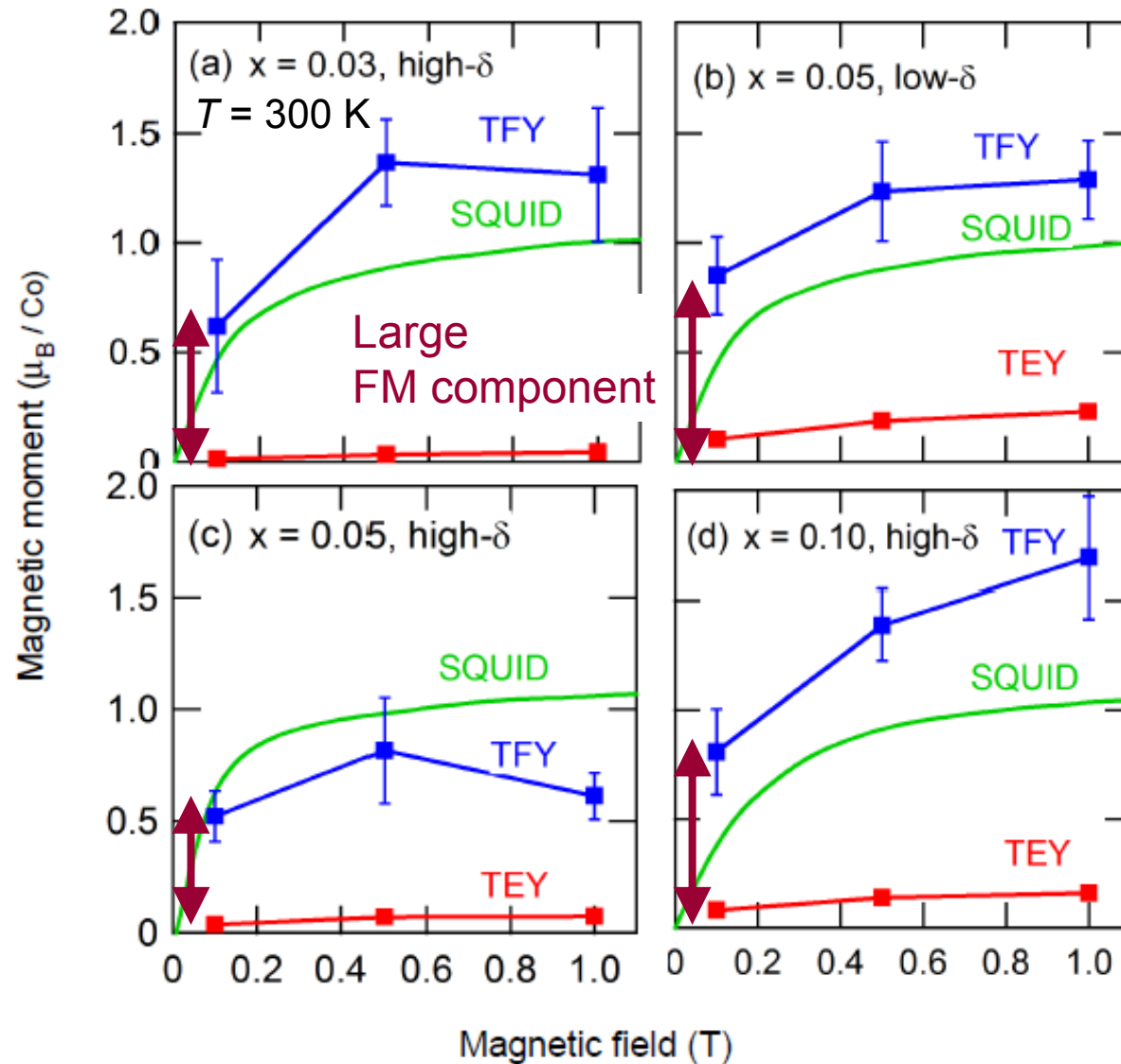
probing depth ~ 100nm ~ sample thickness

Prohibited by ~mm thick substrate

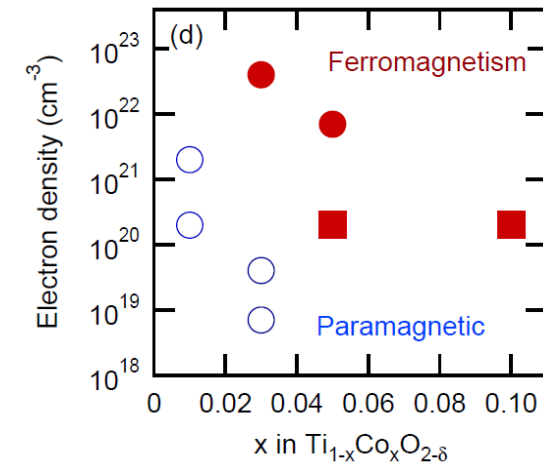
Co 2p XAS and XMCD of $\text{Ti}_{1-x}\text{Co}_x\text{O}_{2-\delta}$ measured by bulk-sensitive TFY mode



XMCD intensity and magnetization vs H for $\text{Ti}_{1-x}\text{Co}_x\text{O}_2$



TFY: bulk-sensitive
 TEY: surface sensitive



Surface dead layer on $\text{Ti}_{1-x}\text{Co}_x\text{O}_2$ film

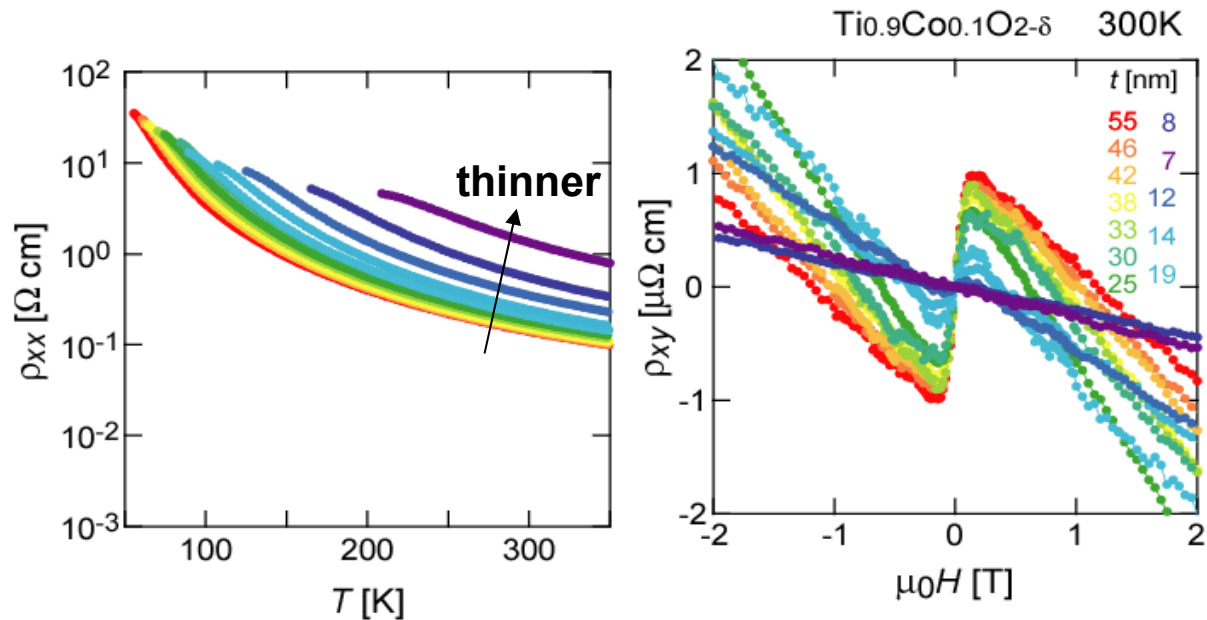
Total fluorescence yield (TFY) mode (probing depth $\sim 100\text{nm}$)

→ Strong XMCD intensity

Total electron yield (TEY) mode (probing depth $\sim 3\text{-}5\text{nm}$)

→ Weak XMCD intensity

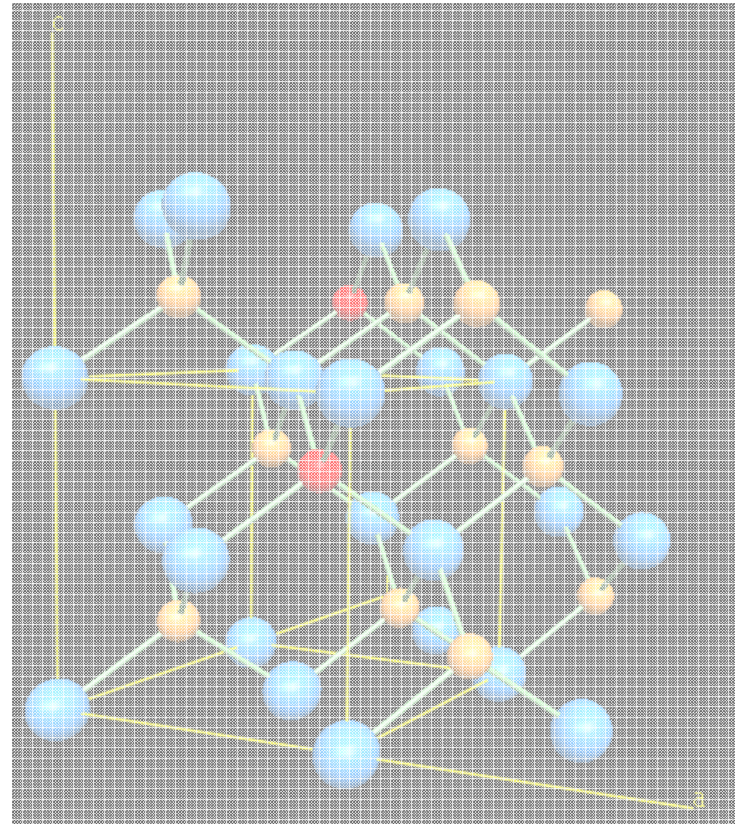
Suppression of AHE for $\text{Ti}_{1-x}\text{Co}_x\text{O}_{2-\delta}$ films



T. Fukumura et al., submitted to APL

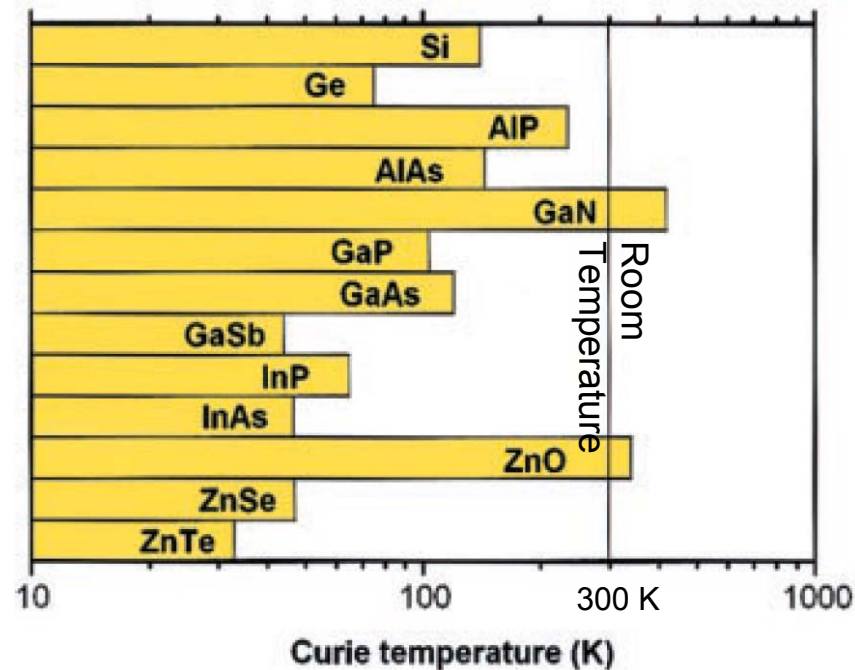
Surface layer of $\sim 5\text{ nm}$ is magnetically dead due to carrier depletion.

ZnO-based DMS



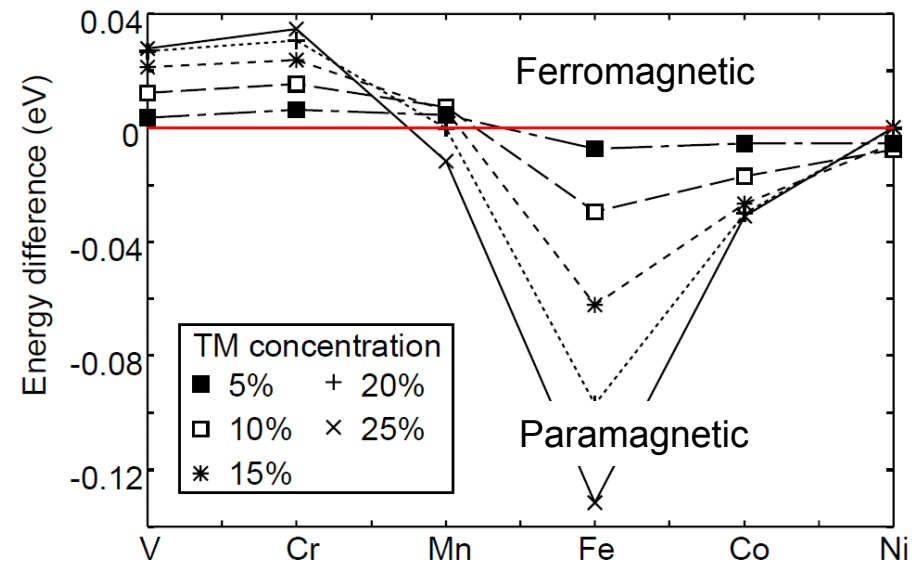
Theoretical prediction of room-temperature ferromagnetism in DMS

T_C of Mn-doped semiconductors in p - d exchange mechanism



T. Dietl et al. Science '00

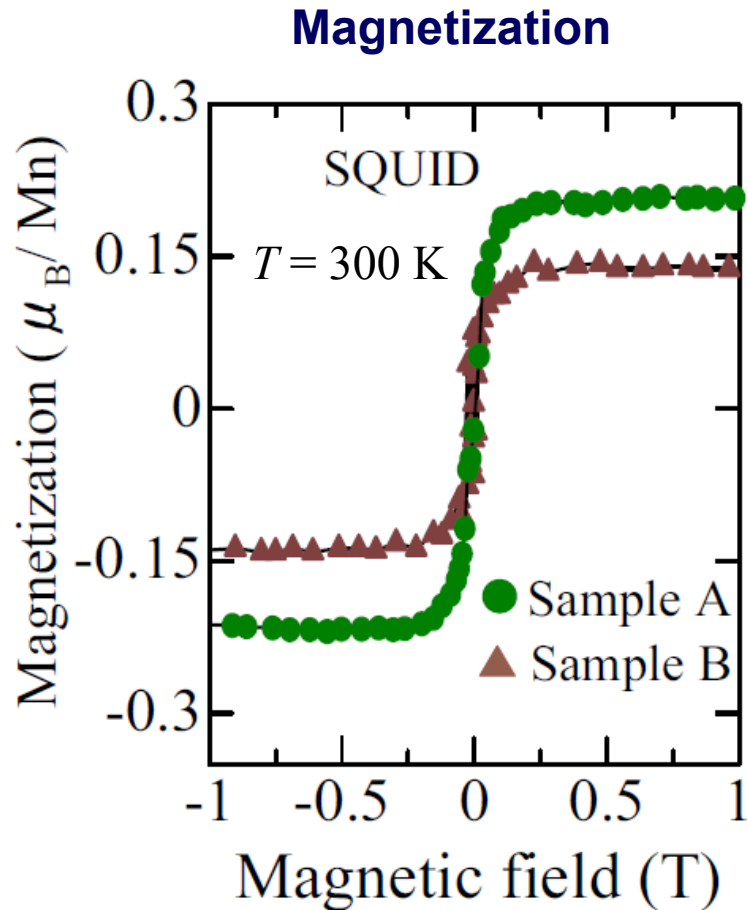
Stability of magnetic states in DMS in double-exchange mechanism



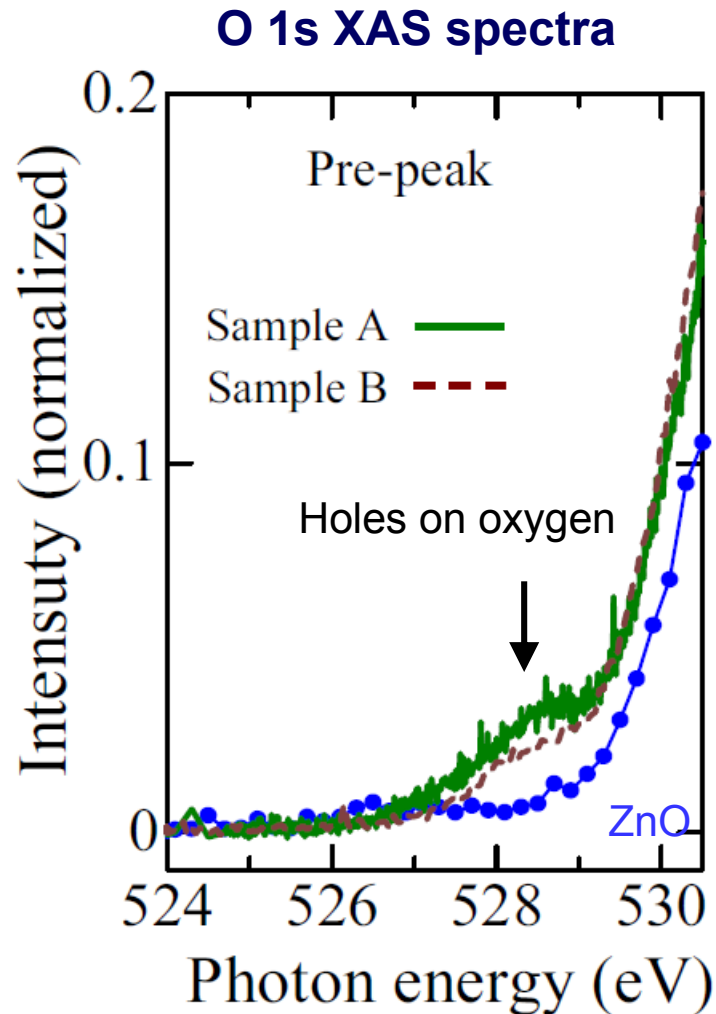
K. Sato et al. JJAP '00.

Wide-gap semiconductors such as ZnO, GaN, and TiO_2 are promising host materials for room-temperature ferromagnetic DMS.

Zn_{0.98}Mn_{0.02}O films prepared under N₂ atmosphere



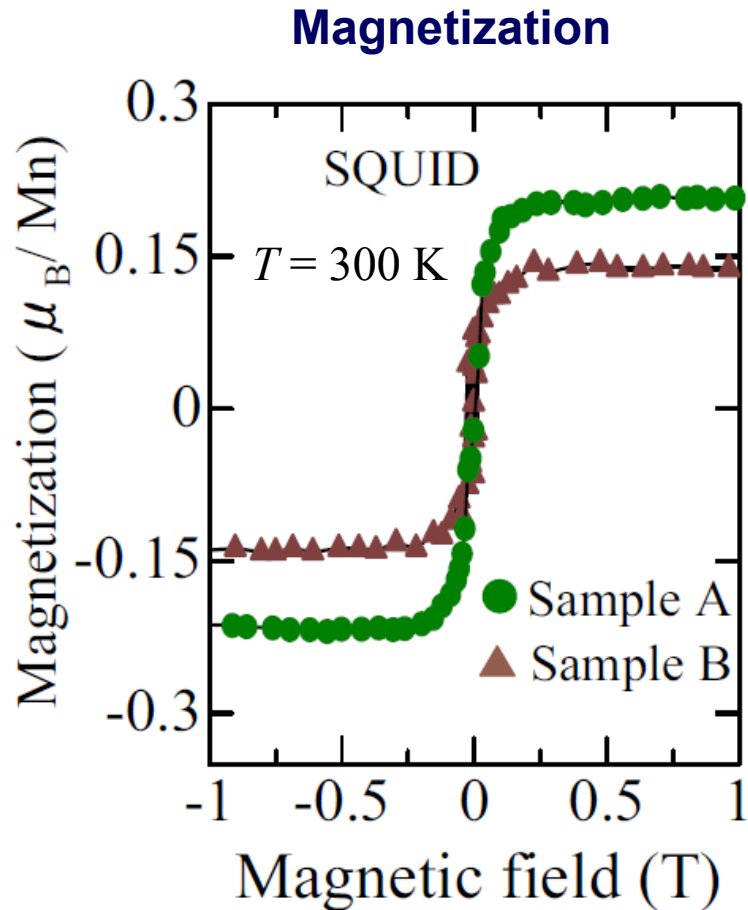
Sample A: $P_{\text{N}_2} = 1.5 \times 10^{-4}$ mbar
Sample B: $P_{\text{N}_2} = 4.0 \times 10^{-4}$ mbar



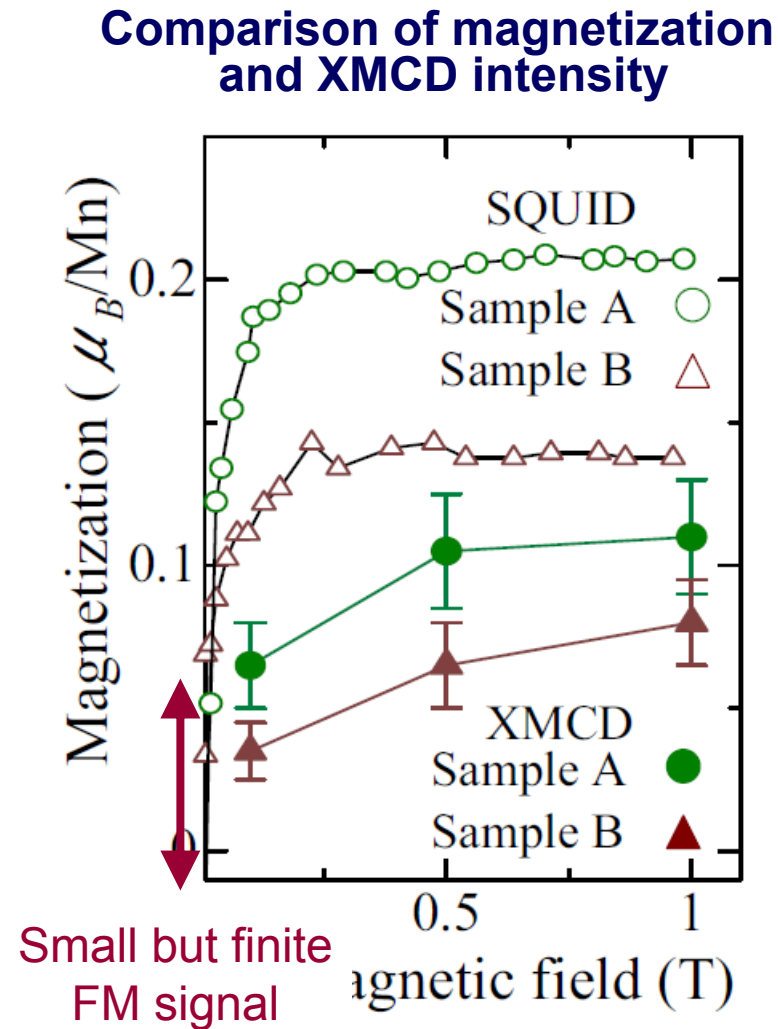
T. Kataoka et al.

cf) P. Sharma et al., Nature Mater '03.

XMCD intensity and magnetization vs H in N-doped $\text{Zn}_{0.98}\text{Mn}_{0.02}\text{O}$ films

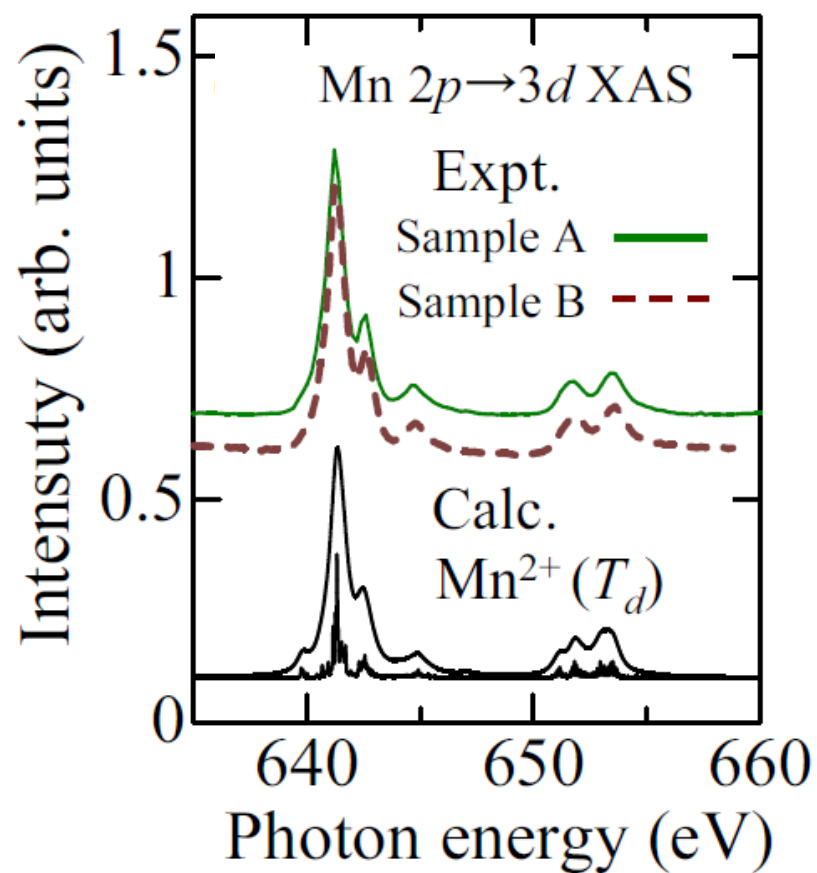


Sample A: $P_{\text{N}_2} = 1.5 \times 10^{-4}$ mbar
Sample B: $P_{\text{N}_2} = 4.0 \times 10^{-4}$ mbar

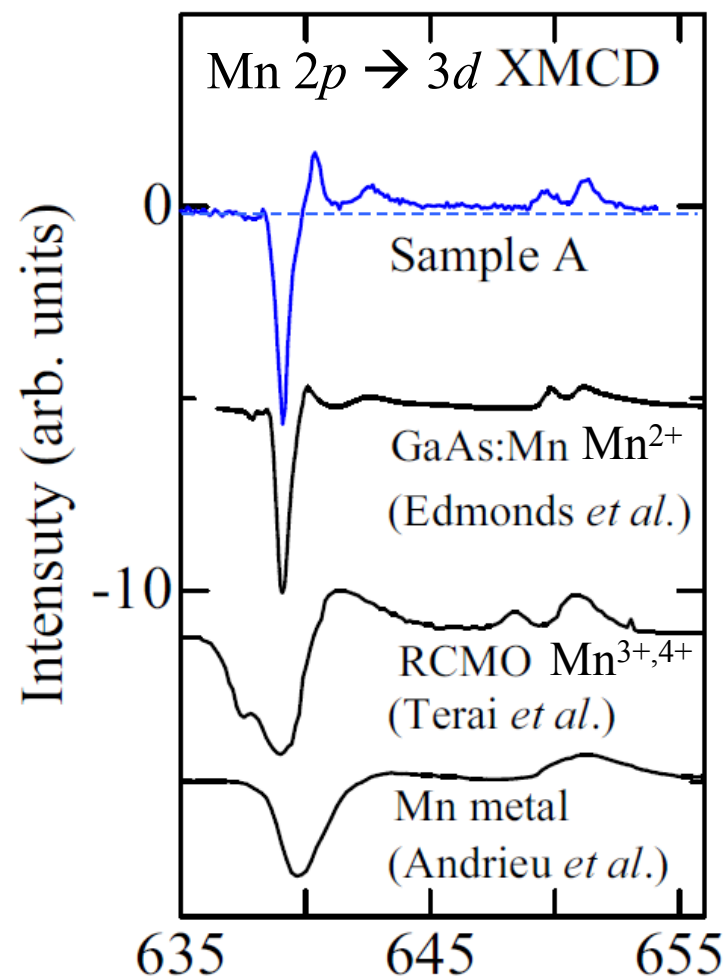


Mn 2p XAS and XMCD of N-doped $\text{Zn}_{0.98}\text{Mn}_{0.02}\text{O}$ films

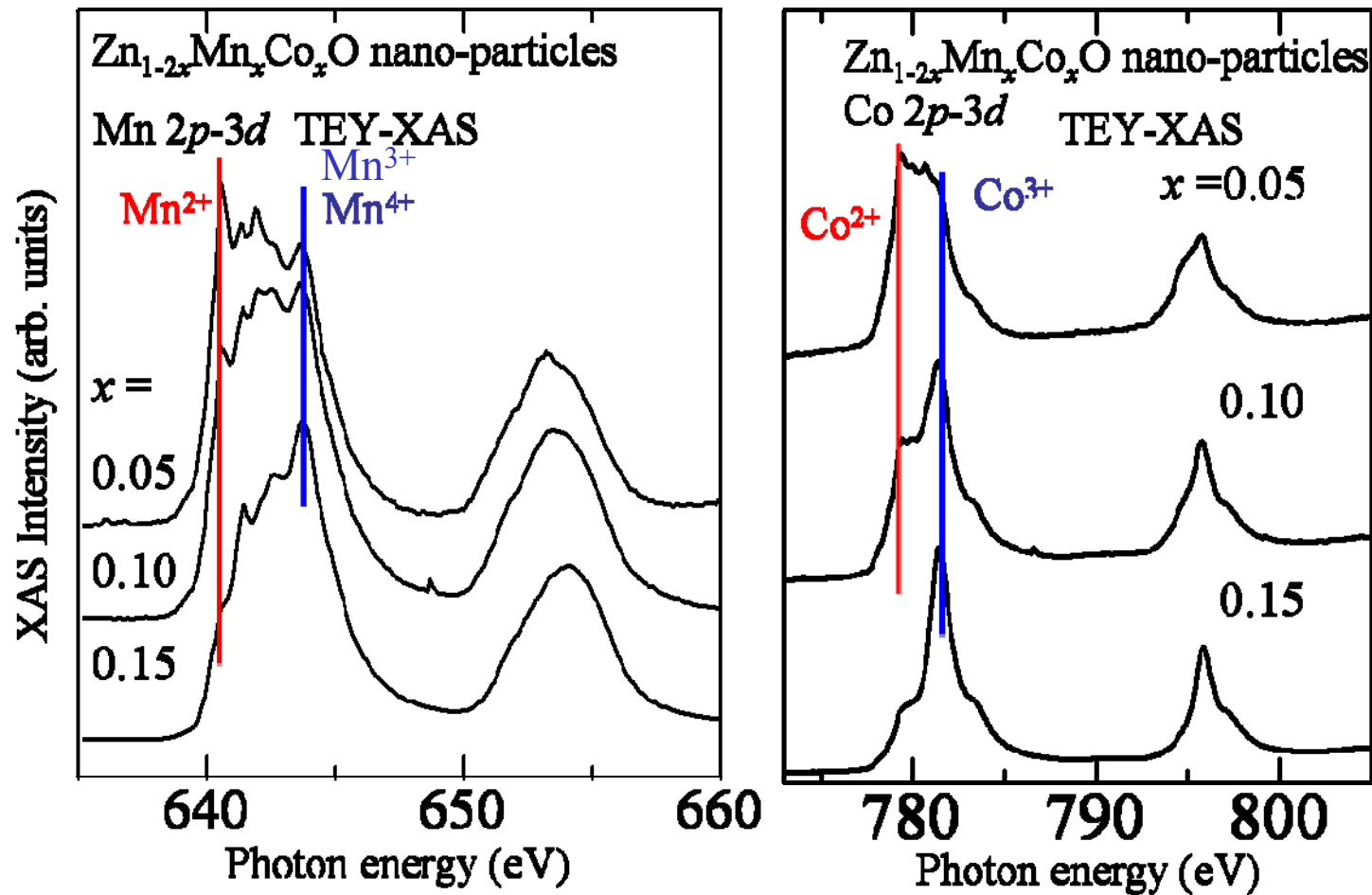
Mn 2p XAS spectra



Mn 2p XMCD spectra



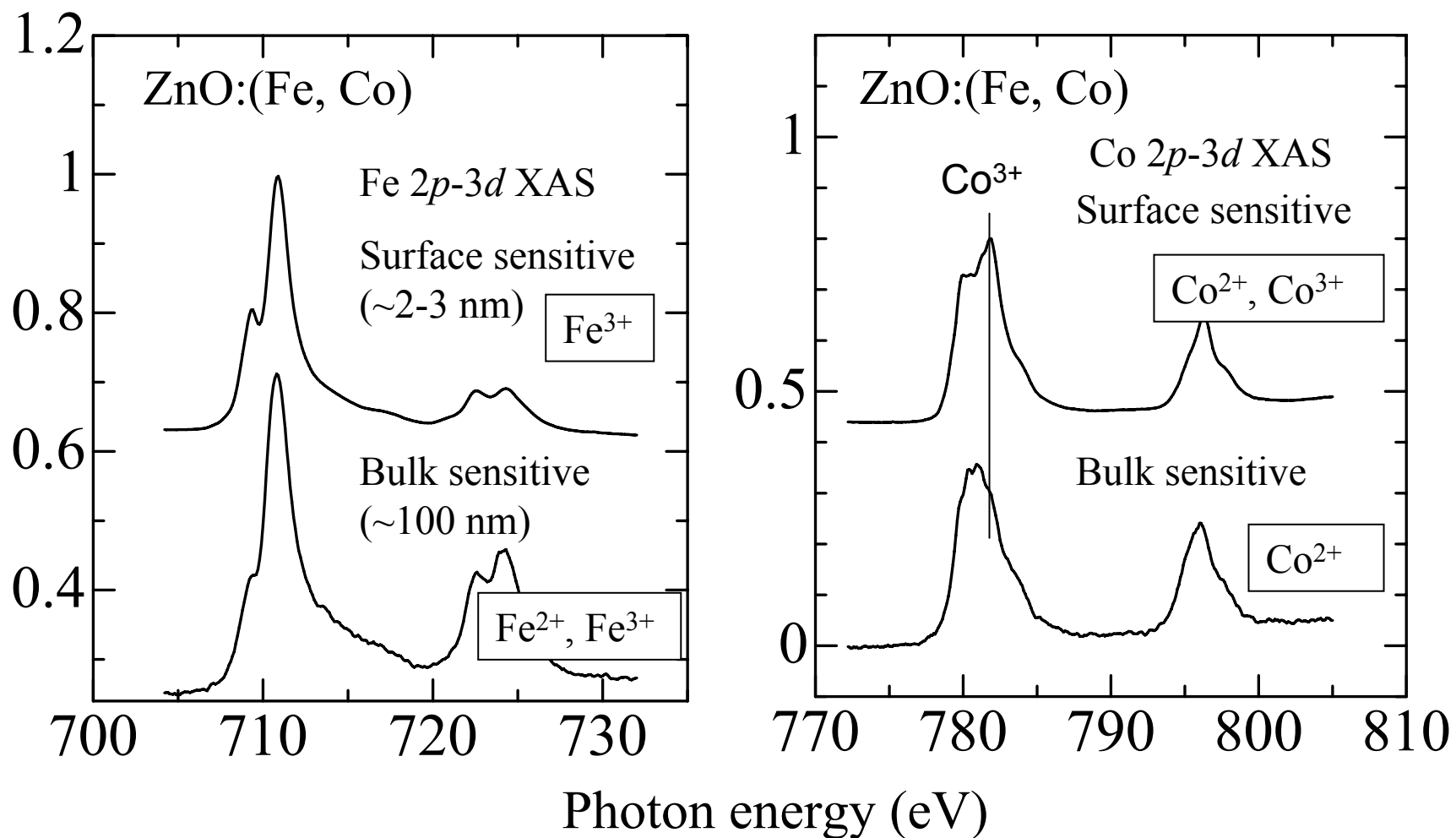
Mn and Co 2p core-level XAS and XMCD of $\text{Zn}_{1-2x}\text{Mn}_x\text{Co}_x\text{O}$ nano-particles



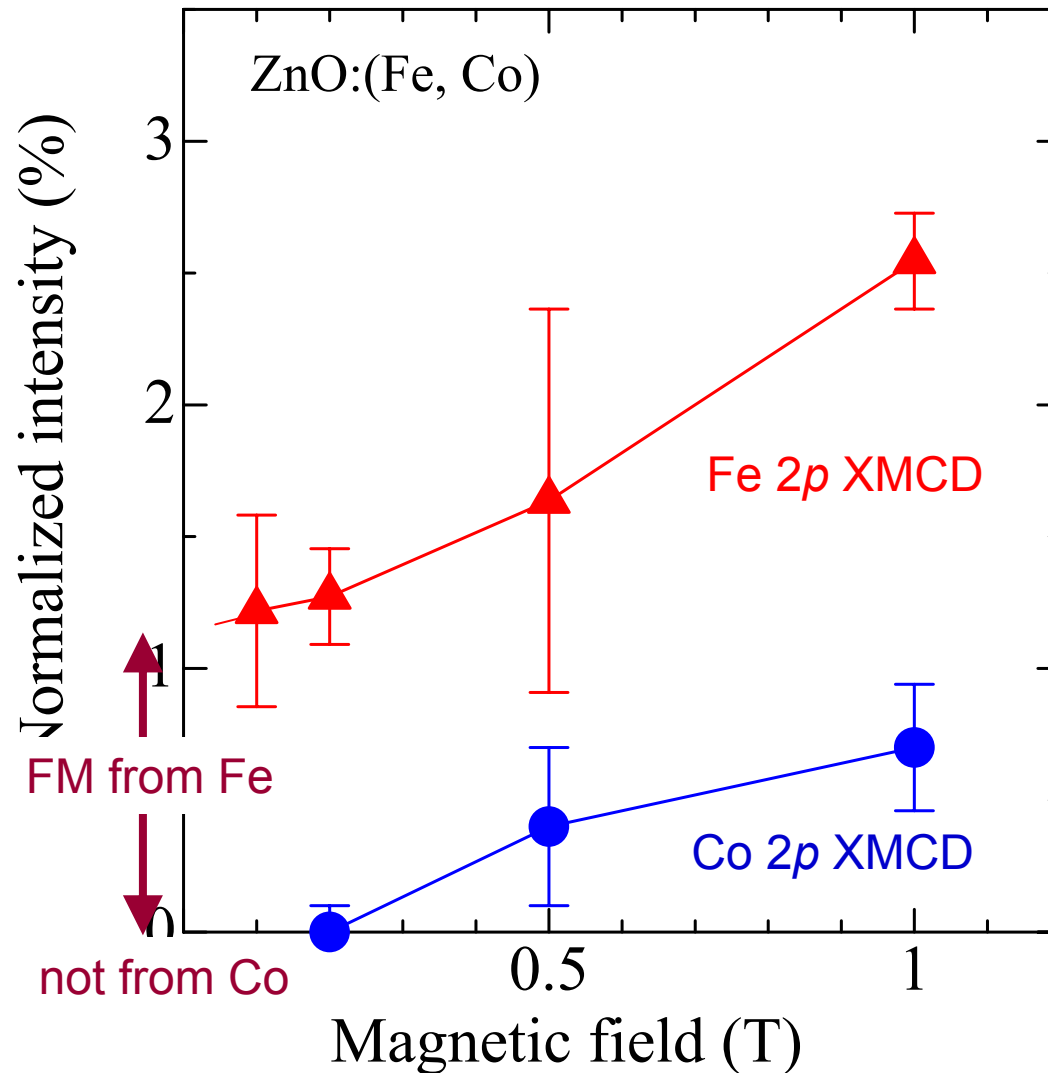
Paramagnetic, unfortunately.

T. Kataoka et al.

Mn and Co 2p core-level XAS and XMCD of $\text{Zn}_{1-2x}\text{Fe}_x\text{Co}_x\text{O}$ nano-particles

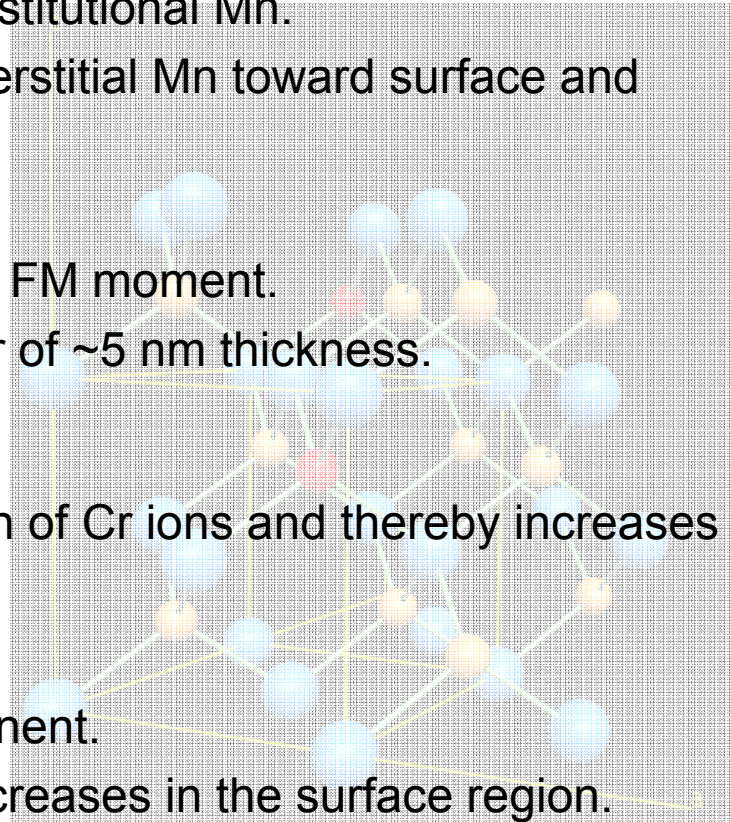


XMCD intensity vs H of $\text{Zn}_{1-2x}\text{Fe}_x\text{Co}_x\text{O}$ nano-particles



Conclusion

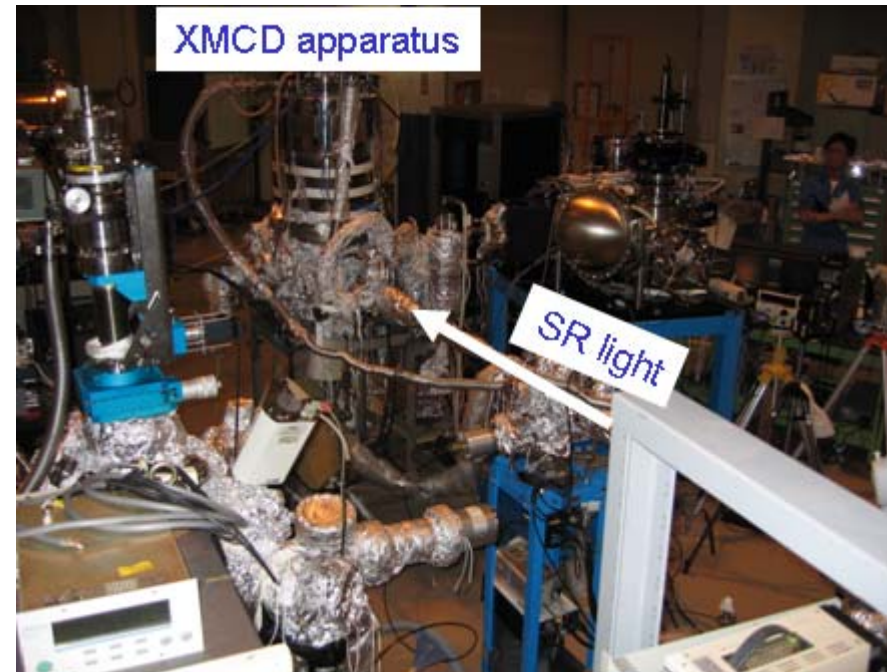
- XMCD of measurements as a function of T and H provide unique and important information about dilute magnetism in semiconductors.
- $\text{Ga}_{1-x}\text{Mn}_x\text{As}$:
 - Interstitial Mn are AFM-coupled to substitutional Mn.
 - Low-temperature annealing expels interstitial Mn toward surface and increase the FM moment in bulk.
- $\text{Ti}_{1-x}\text{Co}_x\text{O}_2$:
 - Co^{2+} ions are responsible for the large FM moment.
 - There exists a magnetically dead layer of ~ 5 nm thickness.
- $\text{Zn}_{1-x}\text{Cr}_x\text{Te}$
 - Cr^{2+} drives inhomogeneous distribution of Cr ions and thereby increases T_C .
- ZnO-based DMS:
 - Films: Hole doping creates FM component.
 - Nano-particles: Valence of TM ions increases in the surface region.



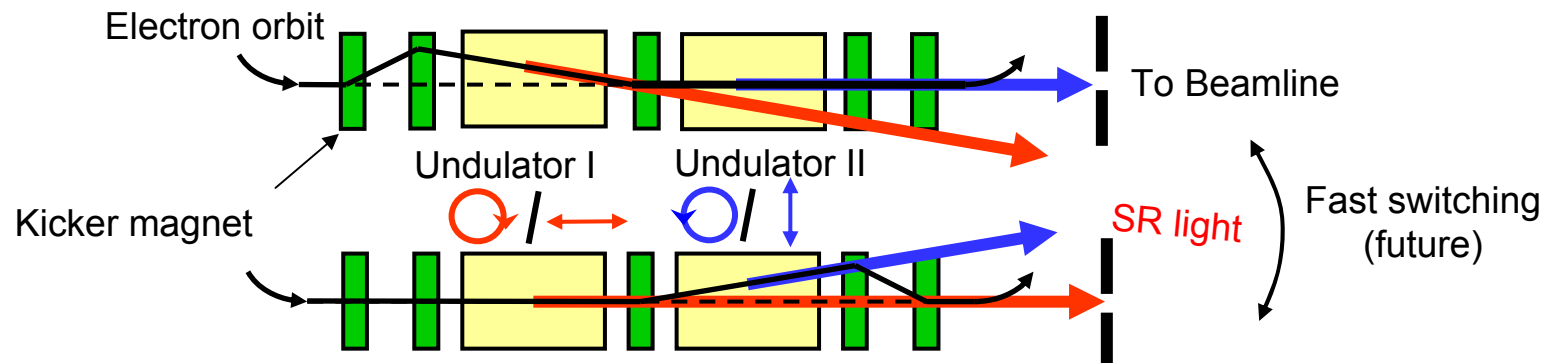
XMCD endstation at BL-16A of Photon Factory (present)



Superconducting magnet, up to 5 T
Low temperature down to ~10 K
Angular-dependent XMCD (L, T)

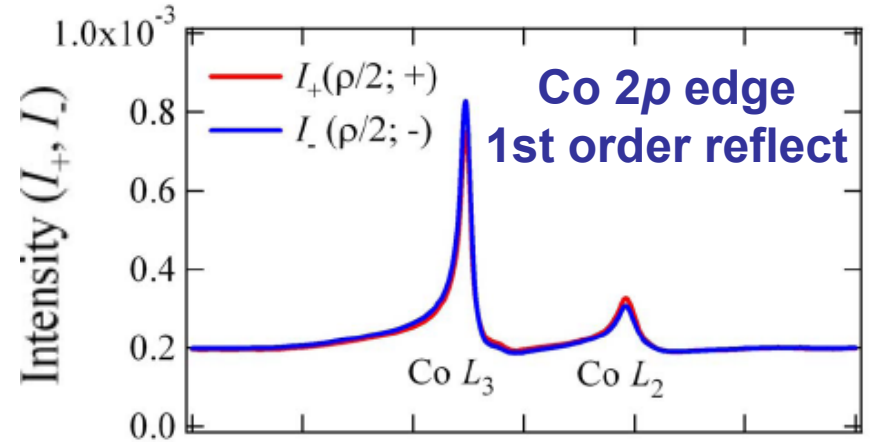
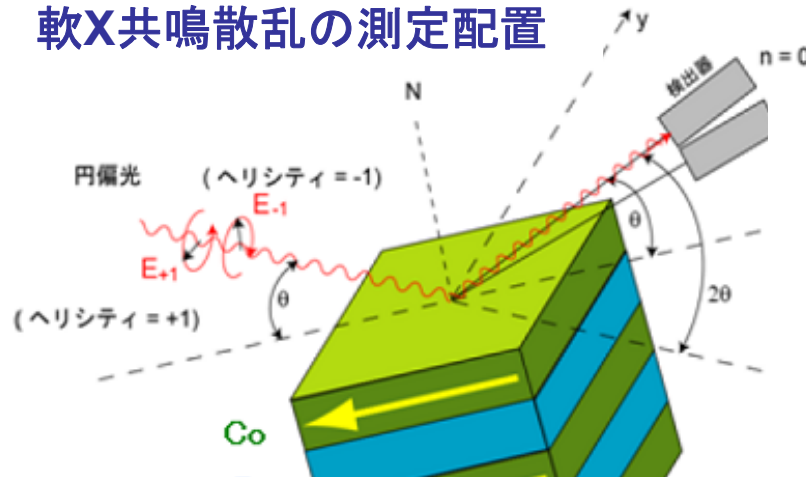


T. Koide et al. Rev. Rev. Sci. Instr. 63, 1462 (1992)

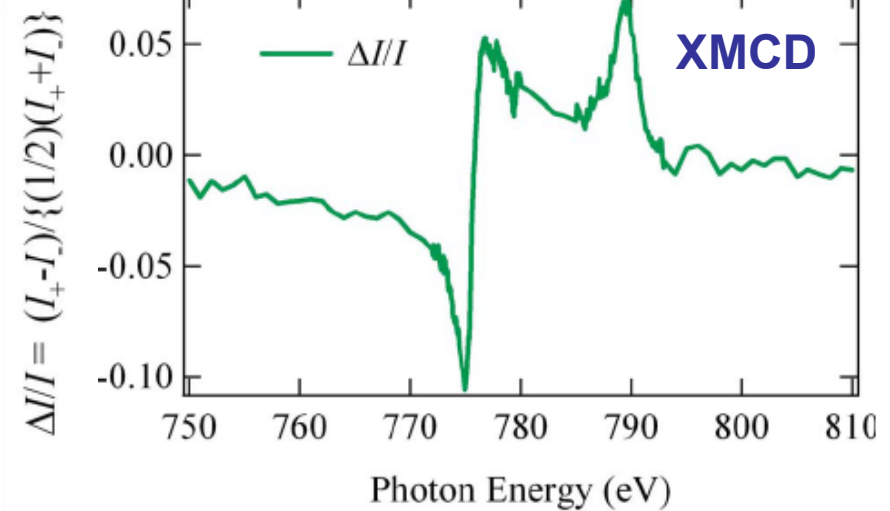
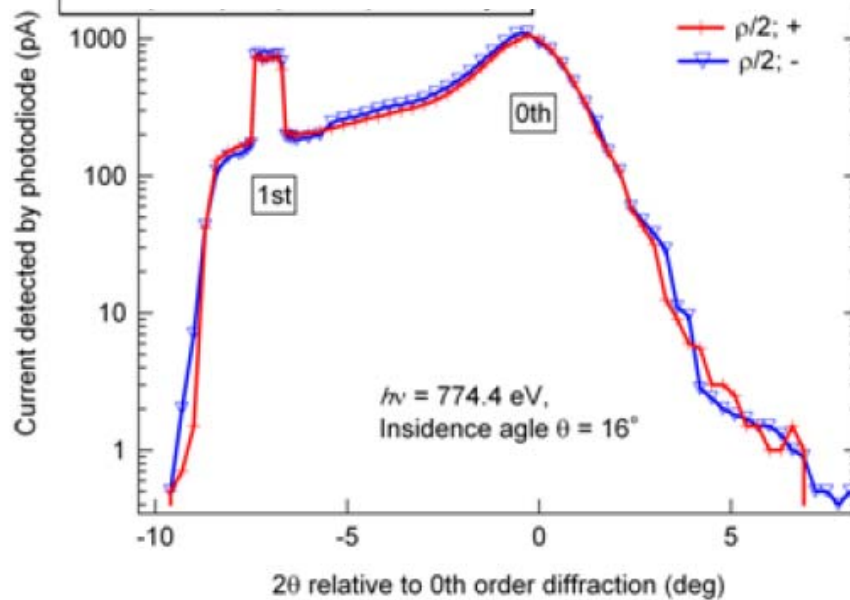


Co(4ML)/Pt(10ML)多層膜に対する予備実験結果

軟X共鳴散乱の測定配置

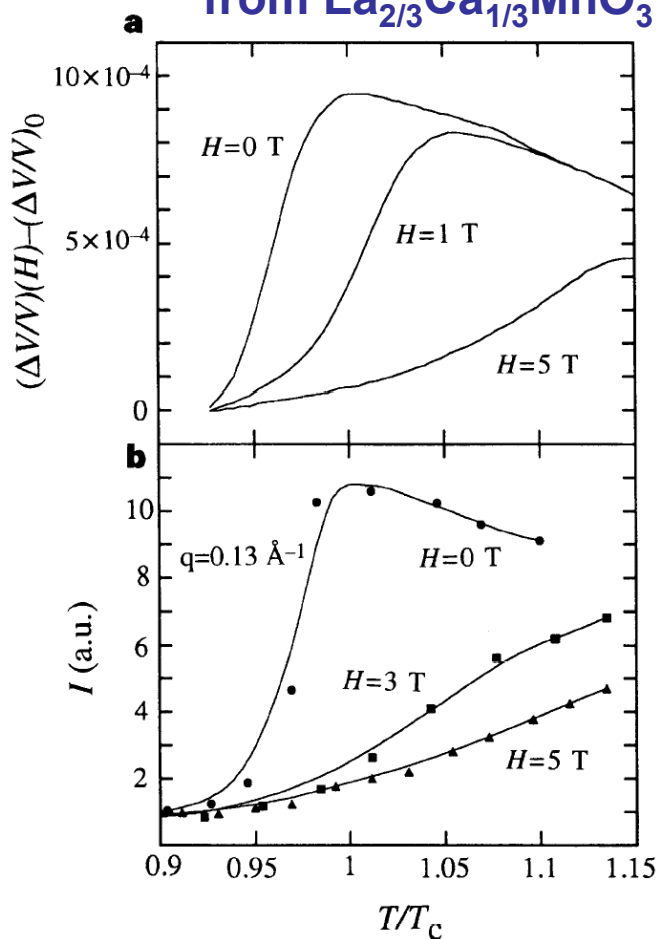


2θ scan at Co 2p edge



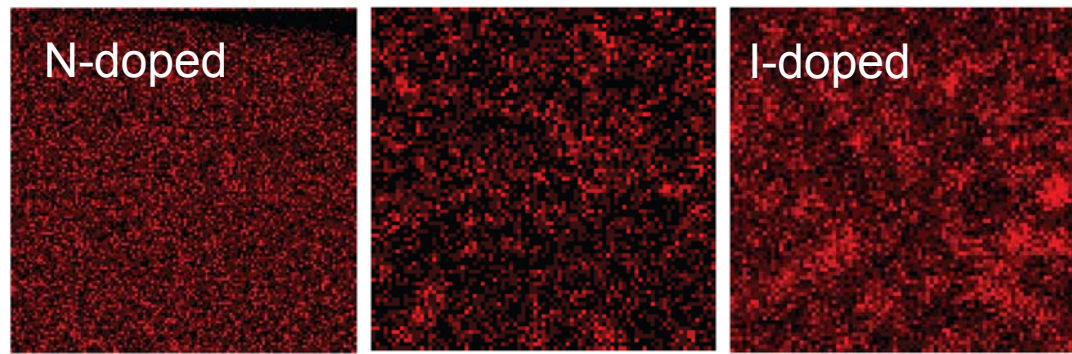
Inhomogeneous chemical and electronic states in high- T_C DMS

Small angle neutron scattering from $\text{La}_{2/3}\text{Ca}_{1/3}\text{MnO}_3$



Ferromagnetic nano-particles
J.M. De Teresa et al., Nature '97

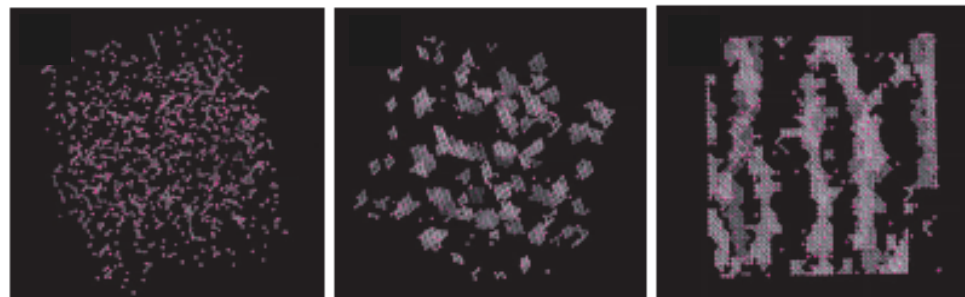
Energy-dispersive X-ray spectroscopy image



uniform T_C low \longleftrightarrow non-uniform T_C high

S. Kuroda et al., Nat. Mater. '07

Spinodal decomposition in high- T_C DMS's



K. Sato et al., JJAP '05, T. Fukushima et al., JJAP '06

→ Cr^{2+} と Cr^{3+} を分離した空間分布, ナノ粒子の電子構造分布

